# Histiocytic Lesions of the Lung

7

Annikka Weissferdt

Histiocytic disorders of the lung cover a wide range of conditions that can involve the lung in isolation or as part of a systemic process. These diseases are caused by proliferative abnormalities of cells of the mononuclear phagocyte system and their principal cell, the histiocyte. Histiocytes comprise a group of immune cells, including antigen-processing macrophages and antigen-presenting dendritic cells [1–3]. Histiocytic disorders, both benign and malignant, are relatively rare in the bronchopulmonary system and can cause a spectrum of conditions with clinical behavior ranging from spontaneous regression to life-threatening syndromes. Some of these disorders present as primary lesions and are of unknown etiology, while others are the result of a histiocytic response to a known cause (Table 7.1). Primary histiocytic disorders discussed in this chapter include Langerhans cell histiocytosis, Erdheim-Chester disease, and Rosai-Dorfman disease, while infections such as Whipple disease or malakoplakia and storage diseases (Gaucher disease, Niemann-Pick disease, Fabry disease) are discussed among the secondary histiocytic disorders. Furthermore, crystal-storing histiocytosis and xanthomatous lesions of the lung will also be discussed. Irrespective of underlying etiology, pathologists should be familiar with the spectrum of histiocytic lesions affecting the pulmonary system as definitive diagnosis often relies on histopathologic confirmation of the disease.

**Table 7.1** Pulmonary histiocytic disorders[a]

| Primary | Secondary | Others |
|---|---|---|
| Langerhans cell histiocytosis | *Storage diseases:*<br>Gaucher disease<br>Niemann-Pick disease<br>Fabry disease | Crystal-storing histiocytosis |
| Erdheim-Chester disease | *Infections:*<br>Whipple disease<br>Malakoplakia | *Xanthomatous lesions:*<br>Xanthoma<br>Juvenile xanthogranuloma |
| Rosai-Dorfman disease | | |

[a]Except malignant histiocytic tumors

## 7.1 Langerhans Cell Histiocytosis

Pulmonary Langerhans cell histiocytosis (PLCH) forms part of a spectrum of conditions characterized by an abnormal proliferation of Langerhans cells. Langerhans cells are members of the family of dendritic cells that function as potent antigen-presenting cells [4]. Langerhans cell histiocytosis (LCH) can involve many organs, including the lungs, bone, skin, pituitary gland, liver, lymph nodes, and thyroid gland [5]. The disease can present as a systemic condition when two or more organs are involved (formerly known as *systemic histiocytosis X*, *Letterer-Siwe disease*, and *Hand-Schüller-Christian syndrome*) or as a localized phenomenon affecting a single organ site (formerly also known as *eosinophilic granuloma*) [1]. Although pulmonary involvement may occur in patient with multisystem disease, in the majority of patients with PLCH, the process is limited to the lung [6, 7]. Systemic LCH is thought to be a neoplastic clonal disorder that primarily affects young children and manifests as a leukemia-like condition with often fatal outcome [8, 9]. In contrast, LCH confined to the lung is typically a benign reactive process in adult patients and strongly linked to cigarette smoking [7, 10]. Recent advances in the understanding of the pathogenesis of Langerhans cell histiocytosis have implicated *BRAF V600E* mutations in the development of the systemic form as well as in a subset of PLCH [11, 12].

### 7.1.1 Clinical Features

Patients with PLCH are typically young adults of whom more than 90% are smokers or ex-smokers [13, 14]. The symptomatology can vary and range from asymptomatic to



A. Weissferdt, *Diagnostic Thoracic Pathology*, https://doi.org/10.1007/978-3-030-36438-0_7

non-productive cough, dyspnea, and pleuritic chest pain or constitutional symptoms, such as weight loss, fever, and night sweats [7, 10, 15]. Hemoptysis is a rare presentation and should prompt search for an underlying neoplasm in the first instance [7, 15]. The most consistent abnormality on pulmonary function tests is decreased carbon monoxide diffusion capacity. Furthermore, patients can show normal, restrictive, obstructive, or mixed patterns on spirometry [14, 16]. PLCH may be complicated by the development of spontaneous pneumothorax and pulmonary hypertension [17, 18]. Classic patterns on HRCT include nodular and cystic changes, mainly affecting the upper and mid zones of the lung and with sparing of the bases and costophrenic angles. Nodules typically measure several millimeters to 2 cm in size and can show central cavitation (Fig. 7.1). As the disease progresses, nodules become less common and are replaced by thin-walled cysts [19, 20]. More unusual findings include the presence of ground glass opacities, lymphadenopathy, or cystic changes involving the lower lobes [19, 21]. If the classic imaging pattern is encountered on HRCT, the diagnosis of PLCH may not require lung biopsy to confirm the diagnosis; however, if imaging shows non-specific patterns pathologic confirmation may become inevitable. Smoking cessation is the most important therapeutic approach and can improve or stabilize disease progression in the majority of patients [22, 23]. Corticosteroids or immunosuppressive therapy has been used in patients with progressive PLCH or systemic disease although the efficacy of such treatment remains disputed [7, 24]. Lung transplantation is reserved for patients with rapid disease progression despite smoking abstinence and immunosuppressant treatment; it has to be noted that PLCH may recur in the transplanted lung, especially if the patient resumes smoking [25, 26]. Most patients with localized PLCH have a good prognosis with estimated 5-year and 10-year overall survival rates of 74% and 64%, respectively [14, 27]. There is a small subgroup of patients however who develop progressive disease with respiratory impairment and end-stage lung disease [10, 28]. Factors associated with such adverse outcome include the extremes of age, prolonged constitutional symptoms, extensive cysts and honeycombing on imaging, markedly reduced diffusion capacity, multiorgan involvement, prolonged steroid administration, obstructive lung function, and development of pulmonary hypertension [6, 28]. Moreover, it has been proposed that the development of neoplastic disease (lung carcinoma and lymphoma) is more frequent in patient with Langerhans cell histiocytosis than in the normal population [29–31].

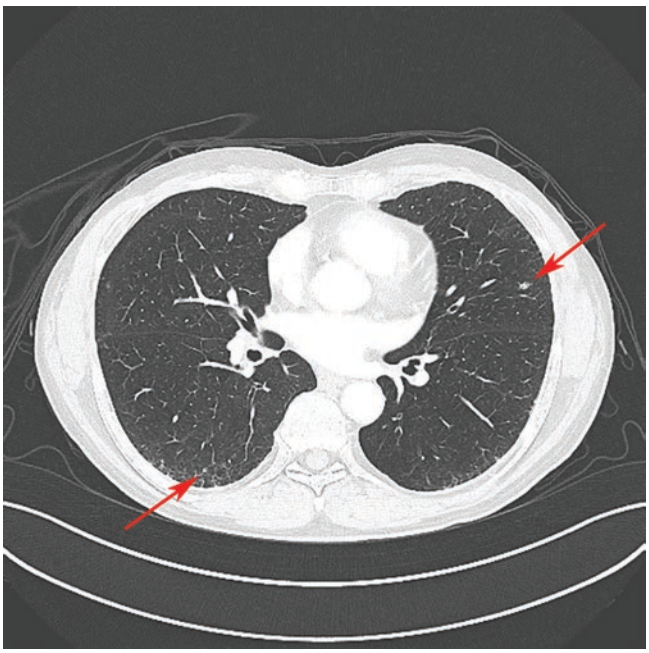

**Fig. 7.1** Computed tomography scan of the chest of a patient with pulmonary Langerhans cell histiocytosis. Note the presence of discrete scattered bilateral pulmonary nodules (arrows)

### 7.1.2 Pathological Features

Nodular parenchymal infiltrates are the main finding on gross examination of open biopsy specimens. The nodules are generally small and measure up to 2 cm in size. In lungs with advanced disease, cystic changes may predominate, especially in the upper and middle zones of the lung. Larger areas of fibrosis and honeycomb changes can be seen in lungs with end-stage lung disease. Microscopically, the nodules in PLCH are small and discrete with preferential arrangement around the small airways (Fig. 7.2a, b). Early lesions are cellular and composed of Langerhans cells, lymphocytes, fibroblasts, variable numbers of eosinophils, and occasional giant cells (Fig. 7.3a–c). A characteristic feature of the nodules in PLCH is the variation of the cellular composition; especially the number of the eosinophils mostly depends on the activity of the lesion (Fig. 7.4). Langerhans cells are characterized by a pale eosinophilic cytoplasm with indistinct cell borders, elongated nuclei, and inconspicuous nucleoli. The nuclei often contain folds and grooves that resemble wrinkled tissue paper (Fig. 7.5). Of note, Langerhans cells in cellular lesions may contain mitotic figures and should not be mistaken for malignant cells (Fig. 7.6). In some cases, the cellular nodules can obliterate the underlying small airway. As the disease progresses, the nodules enlarge and may attain a size of up to 2 cm. Cavities may develop within these nodules and with time the cellular infiltrate is replaced by a fibroblastic proliferation leading to stellate-shaped scars with finger-like extensions and cyst formation (Fig. 7.7a–c). In this stage,

the characteristic cellular infiltrate may not be identified any longer, and only scattered scars remain (so-called burned-out PLCH) (Fig. 7.8). It is common to find lesions in all stages of development in the same lung specimen and cellular nodules may be found adjacent to stellate scars. Other pathological findings include other smoking-related conditions including respiratory bronchiolitis, a desquamative interstitial pneumonitis (DIP)-like reaction characterized by collections of pigmented macrophages in the alveolar spaces surrounding individual lesions, and emphy-

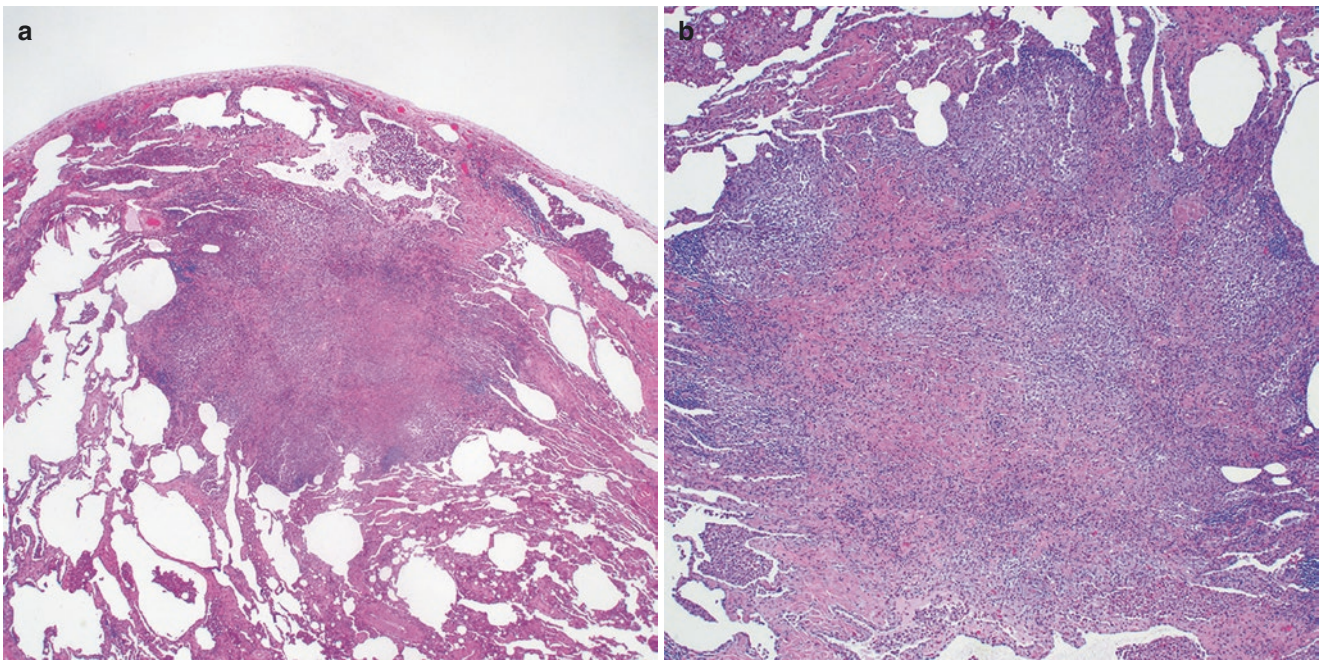


**Fig. 7.2** (**a**) Low power view of a typical cellular nodular lesion in the lung parenchyma in Langerhans cell histiocytosis; (**b**) higher magnification reveals a solid nodule composed of varying degrees of inflammatory cells and fibrous tissue

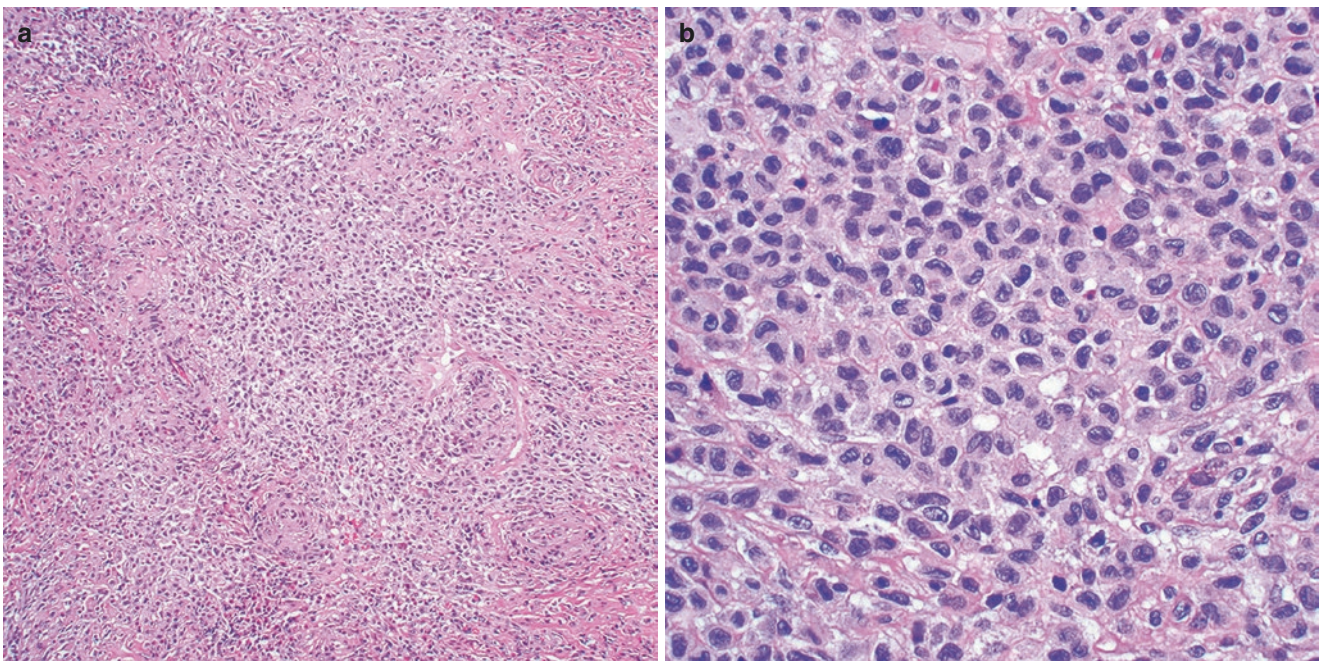


**Fig. 7.3** (**a**) Early cellular lesion in Langerhans cell histiocytosis; (**b**) high power view of a cellular nodule shows numerous histiocytes; (**c**) these nodules can contain occasional giant cells

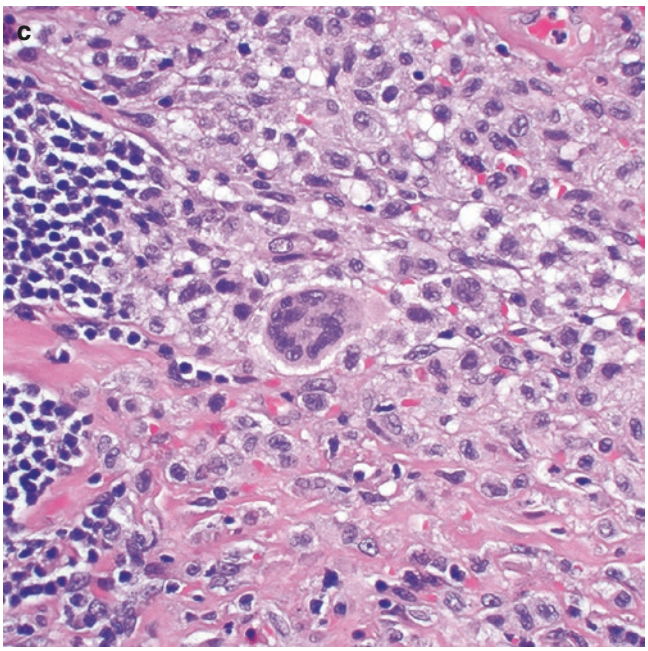


**Fig. 7.3** (continued)

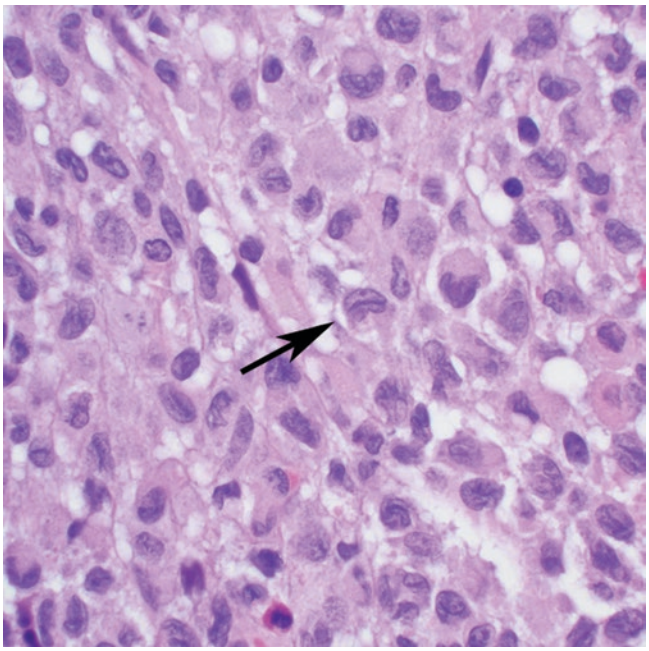

**Fig. 7.5** High power magnification of individual Langerhans cells demonstrates characteristic nuclear grooves and folds (arrow) imparting a crumpled tissue paper appearance

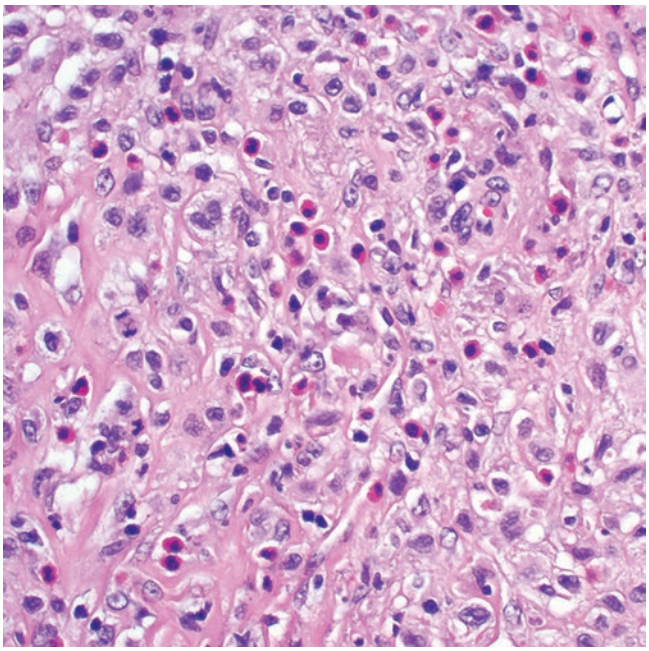

**Fig. 7.4** A characteristic finding in pulmonary Langerhans cell histiocytosis is the presence of variable numbers of eosinophils

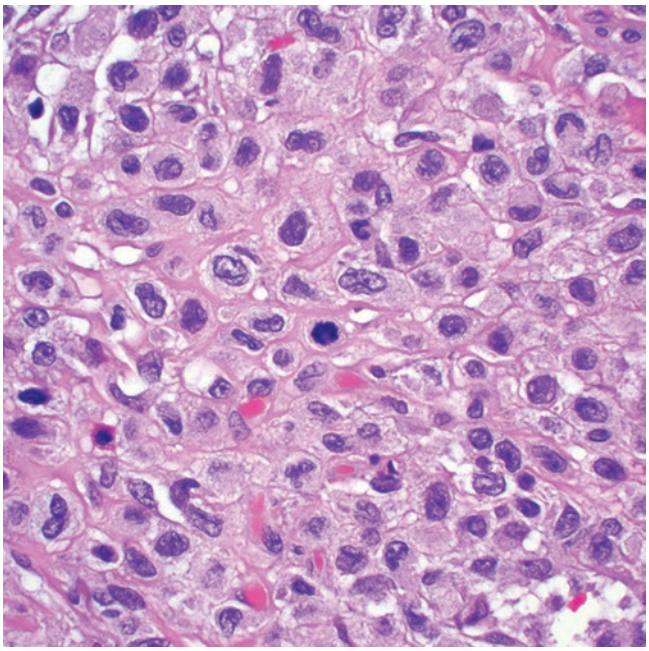

**Fig. 7.6** Mitotic figure in a cellular lesion in pulmonary Langerhans cell histiocytosis

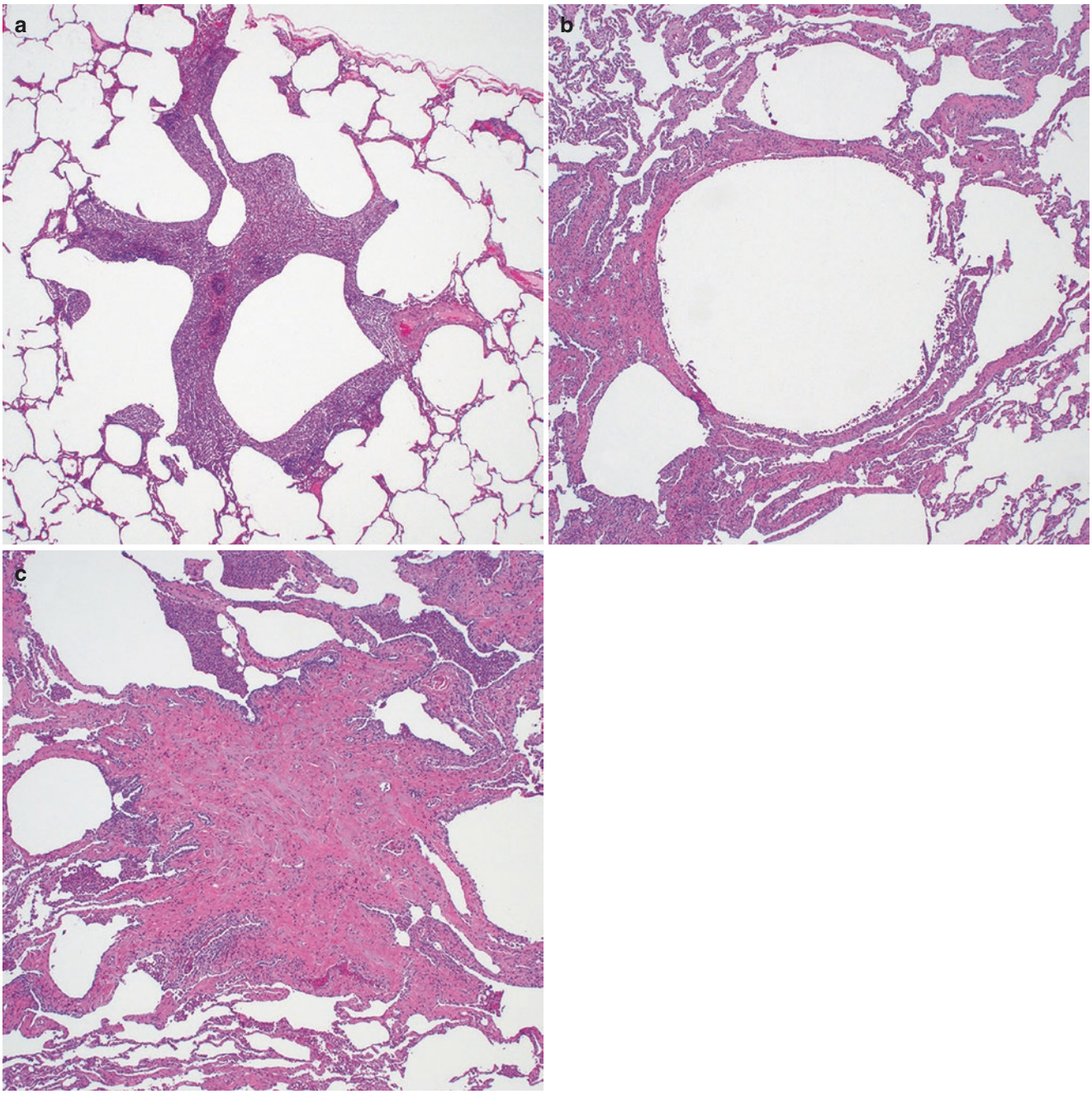


**Fig. 7.7** (**a**) Cellular nodule showing beginning cavitation in pulmonary Langerhans cell histiocytosis; (**b**) cystic changes are often seen in long-standing disease; (**c**) eventually, the nodules undergo fibrosis leaving stellate-shaped scars

sematous changes (Fig. 7.9a, b). In progressive disease, the scars may become larger and confluent and form more extensive areas of fibrosis leading to end-stage lung disease with honeycombing [10, 15, 23, 32] (Fig. 7.10). In some cases, a vasculopathy characterized by intimal fibrosis and medial hypertrophy of pulmonary arteries can develop leading to clinical signs and symptoms of pulmonary hypertension [33] (Fig. 7.11).

### 7.1.3 Laboratory, Immunohistochemical, Ultrastructural, and Molecular Features

The diagnosis of active PLCH can be supported by evaluation of bronchoalveolar lavage (BAL) fluid. A proportion of CD1a-positive Langerhans cells of 5% or greater is thought to be supportive of the diagnosis [34], although the test has been criticized for its lack of sensitivity. Besides CD1a,

other immunohistochemical markers that can highlight Langerhans cells are S100 protein and langerin (CD207), the latter being expressed exclusively in Langerhans cells [35] (Table 7.2) (Fig. 7.12a–c). Ultrastructurally, the hallmark of Langerhans cells is the Birbeck granule, a rod-shaped intercellular structure that is shaped like a tennis racket [36]. Although highly characteristic, identification of Birbeck granules via electron microscopy is hardly performed nowadays as the combination of clinical, morphological, and immunohistochemical findings usually allows

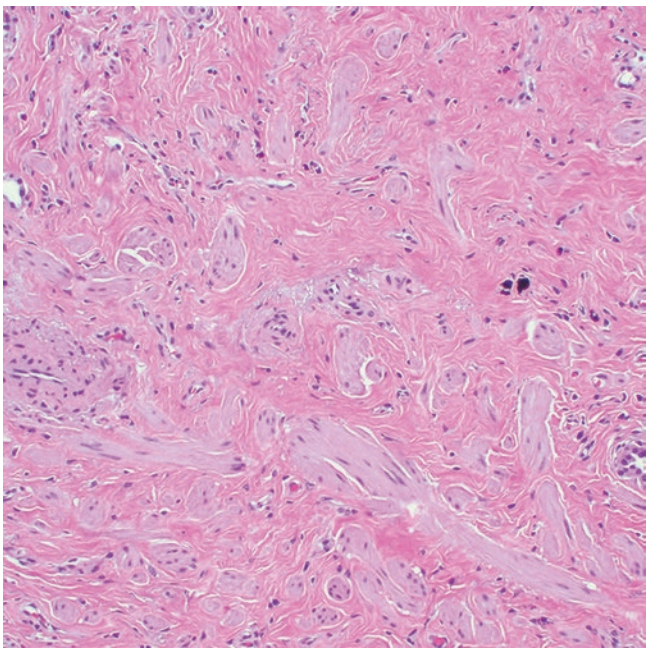

**Fig. 7.8** The scars in pulmonary Langerhans cell histiocytosis are paucicellular and mainly composed of collagen; the characteristic cellular infiltrate is not identified in this stage of the disease

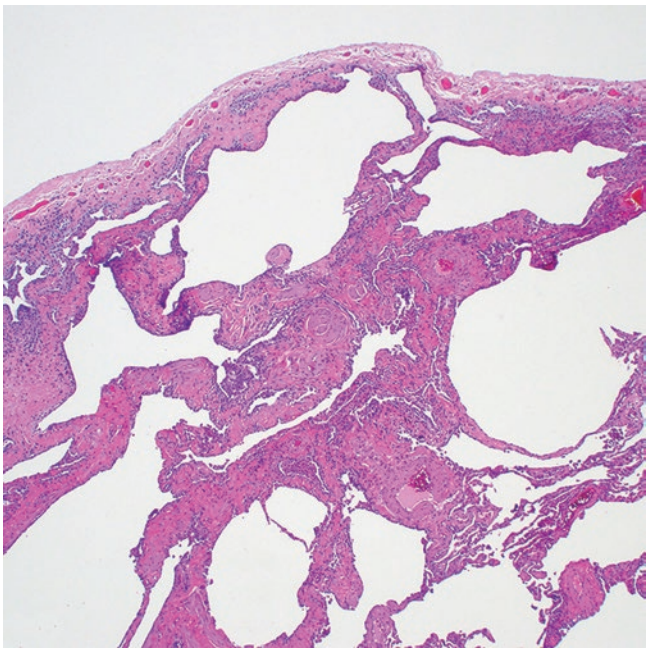

**Fig. 7.10** In long-standing Langerhans cell histiocytosis, areas of end-stage lung disease with scarring and architectural distortion may develop

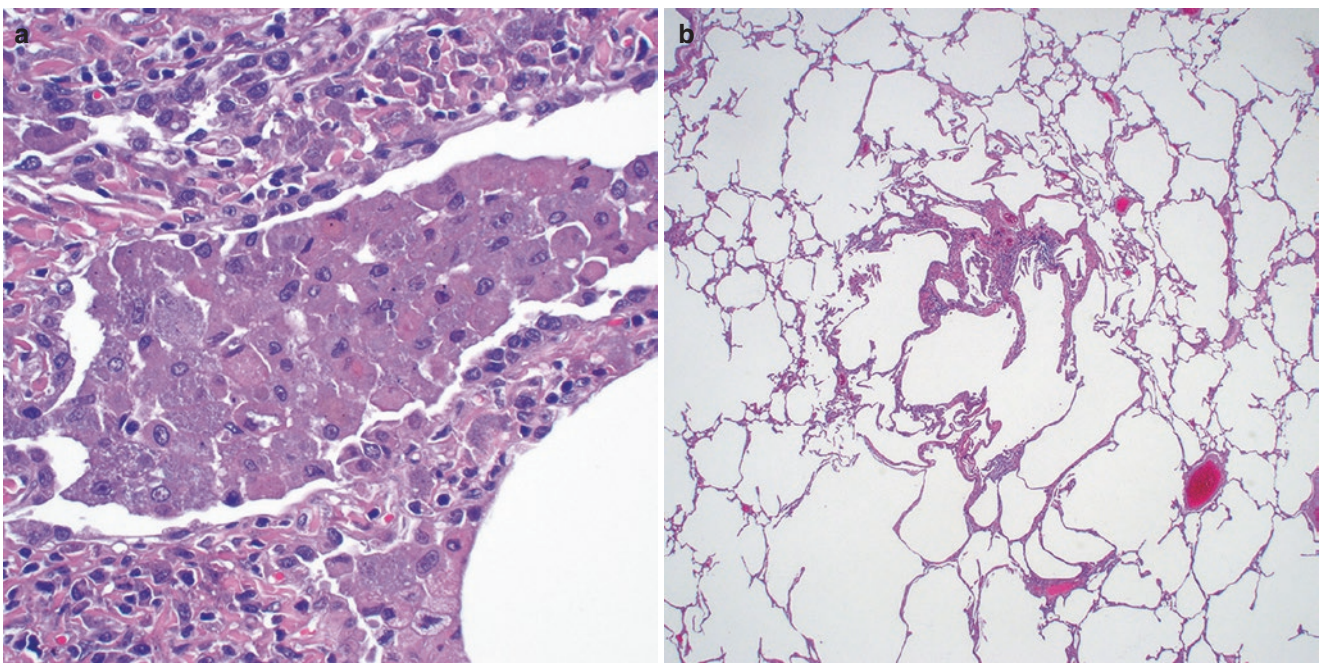


**Fig. 7.9** (**a**) The alveolar spaces surrounding the nodular lesions in pulmonary Langerhans cell histiocytosis often show a desquamative interstitial pneumonitis-like reaction; (**b**) emphysematous changes are also not uncommon

confident diagnosis of the disease. In recent years, a causative role for *BRAF V600E* mutations has been observed in the pathogenesis of pediatric and adult cases of Langerhans cell histiocytosis as well as in a subset of cases of PLCH [11, 12]. Whether in such cases treatment with MAPKinase pathway inhibitors is indicated remains to be elucidated.

### 7.1.4 Differential Diagnosis

In the appropriate clinical and radiological context, the diagnosis of PLCH is usually straightforward. Surgical lung biopsy, preferentially in form of open lung biopsy or cryobiopsy, is indicated when the clinical or imaging findings are inconclusive. On a histological level, the differential diagnosis for PLCH depends on the predominance of cellular versus fibrotic lesions. The cellular form may be confused with DIP, chronic eosinophilic pneumonia, or Hodgkin disease. True DIP can be separated from the DIP-like reaction in PLCH based on the interstitial location of the cellular infiltrates in PLCH, in contrast to the intraalveolar location in DIP which is thought to be due to the effects of smoking. Likewise, in chronic eosinophilic pneumonia, an accumulation of eosinophils will be found in the intraalveolar spaces unlike the interstitial distribution in PLCH. Hodgkin disease of the lung may enter the differential diagnosis based on its mixed cellular composition that includes histiocytes and eosinophils among others. In Hodgkin disease, however, characteristic atypical Reed-Sternberg cells can be identified; such cells are not seen in PLCH. The fibrotic form of PLCH may be mistaken for other forms of interstitial lung disease, such as usual interstitial pneumonia (UIP). In PLCH, the fibrosis is typically symmetrical, and uninvolved lung parenchyma can appear normal. In contrast, the fibrosis in UIP is generally larger and more irregular, and the surrounding parenchyma will contain a mononuclear cell infiltrate devoid of clusters of Langerhans cells in the interstitium. In difficult cases, application of immunohistochemical markers to identify Langerhans cells may become necessary.

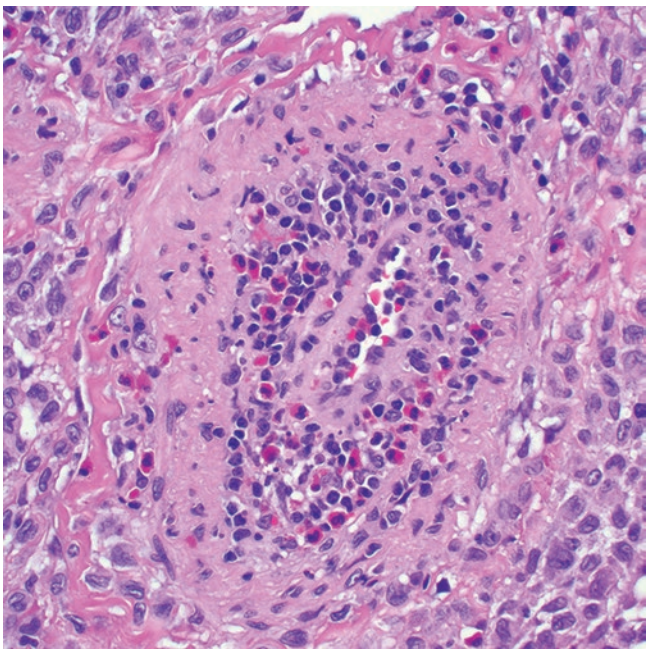

**Fig. 7.11** In some cases, the vasculature may be involved in pulmonary Langerhans cell histiocytosis which may eventually lead to the development of pulmonary hypertension

## 7.2 Erdheim-Chester Disease

Erdheim-Chester disease (ECH) is a rare systemic histiocytic disorder that was first described by Chester in 1930 [37]. The disease affects middle-aged to older adults, and the most common clinical manifestation is bone involvement, characterized by a symmetric pattern of osteosclerosis in the metaphysis or diaphysis of long bones caused by an infiltrate of foamy histiocytes. Bone pain is the most common presenting symptom. Extraskeletal manifestations develop in 50% of patients including involvement of the retroperitoneum, kidney, central nervous system, skin,

**Table 7.2** Key features of primary histiocytic disorders of the lung

| | Langerhans cell histiocytosis | Erdheim-Chester disease | Rosai-Dorfman disease |
|---|---|---|---|
| Etiology | Smoking | Unknown | Unknown |
| Radiology | Nodular and cystic changes | Interlobular septal and pleural thickening, ground glass changes | Circumscribed masses or diffuse bilateral lesions |
| Histology | Cellular nodules composed of Langerhans cells, lymphocytes, fibroblasts, eosinophils; fibrotic lesions composed of stellate-shaped scars | Proliferation of large foamy histiocytes involving interlobular septa, bronchovascular bundles, and pleura | Diffuse infiltrate of voluminous histiocytes, lymphocytes, plasma cells, neutrophils, and eosinophils; emperipolesis |
| IHC | S100+, CD1a+, langerin+, CD68+ | S100+/−, CD1a−, langerin−, CD68+ | S100+, CD1a−, langerin−, CD68+ |
| EM | Birbeck granules | Non-specific | Non-specific |
| Molecular | *BRAF* mutations (subset) | *BRAF* mutations | None |
| Prognosis | Good with smoking cessation | Variable | Good |

*IHC* immunohistochemistry, *EM* electron microscopy

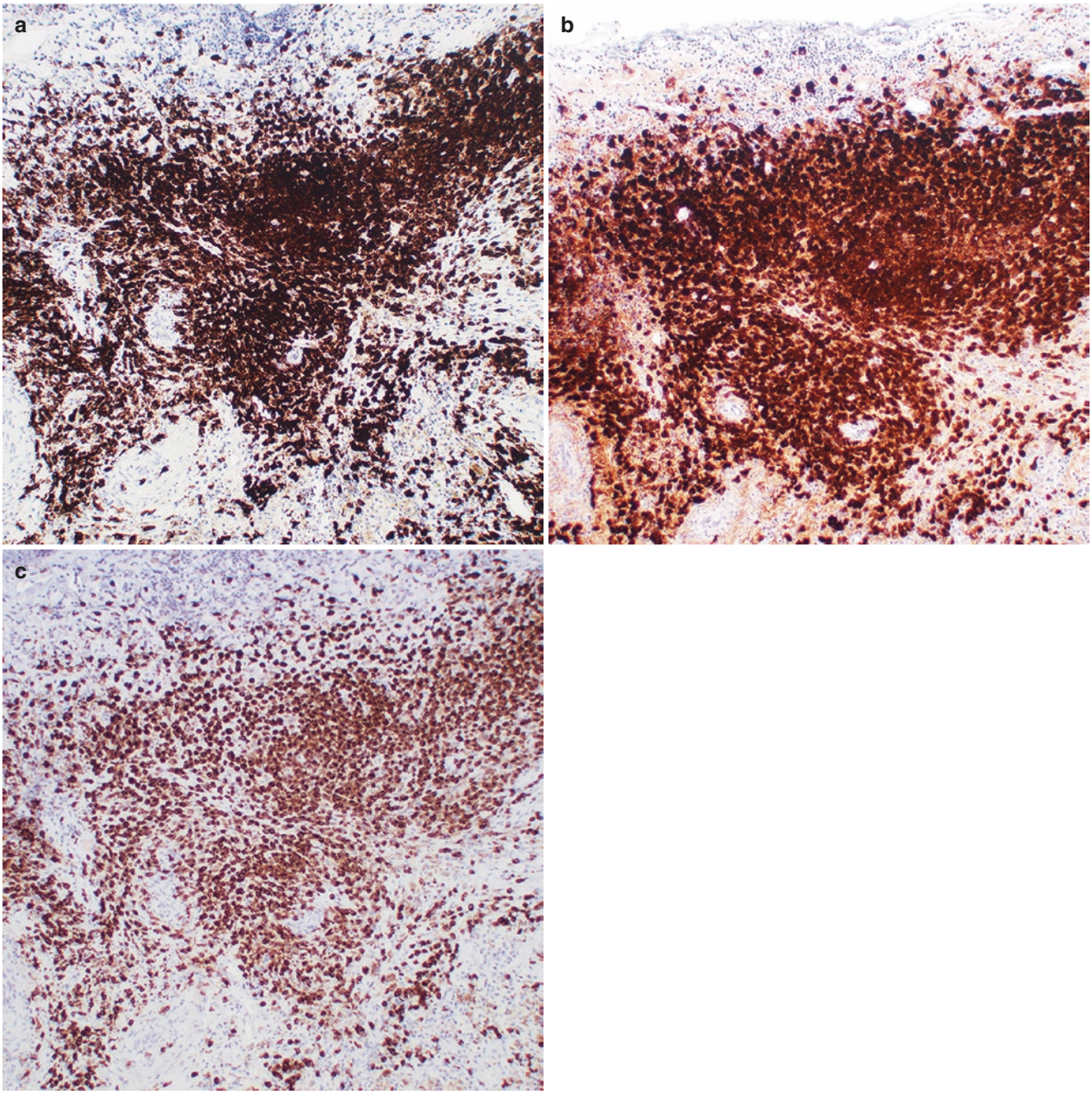


**Fig. 7.12** The immunophenotype of Langerhans cell histiocytosis is characterized by reactivity of the cellular infiltrate for (**a**) CD1a, (**b**) S100 protein, and (**c**) langerin

heart, pituitary, and orbit [38, 39]. Involvement of the lung is seen in up to 25% of patients [10]. The clinical course largely depends on the extent and distribution of the disease and ranges from isolated benign bone lesions to life-threatening systemic disease. The pathogenesis of ECD is poorly understood, however recent identification of activating *BRAF V600E* mutations in about 50% of all cases supports a clonal disease process rather than a reactive etiology and has provided novel treatment approaches with *BRAF* inhibitors [41, 42]. Contrary to Langerhans cell histiocytosis, an association with smoking has not been identified.

### 7.2.1 Clinical Features

Patients with lung involvement by ECD are usually middle-aged or older adults with a mean age in the 6th decade. Generally, patients are older than 40 years of age. Men and women are equally affected [40]. The signs and symptoms of pulmonary ECD include progressive dyspnea over a period of months to years. Pulmonary function studies usually show a restrictive defect, and carbon monoxide diffusion capacity is reduced in most patients [38]. Radiographic changes include diffuse interstitial infiltrates and pleural thickening. HRCT findings that would support

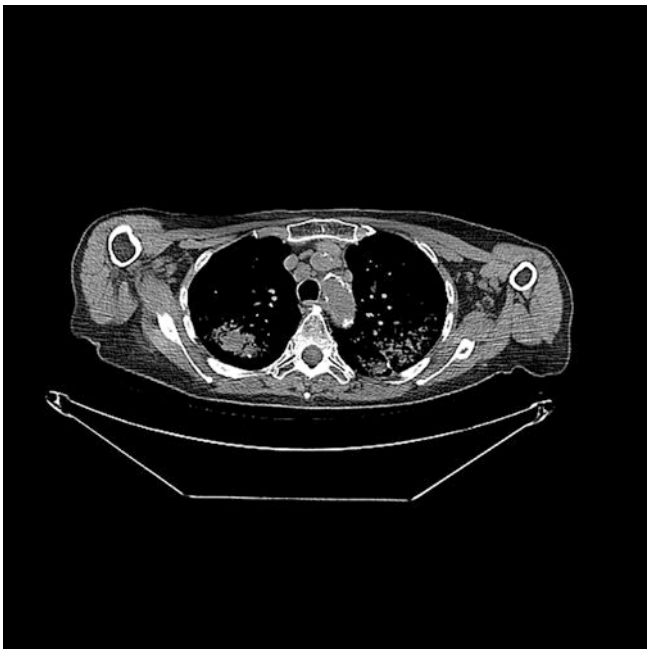

**Fig. 7.13** Chest computed tomography scan of a patient with Erdheim-Chester disease shows bilateral consolidative opacities involving the lungs

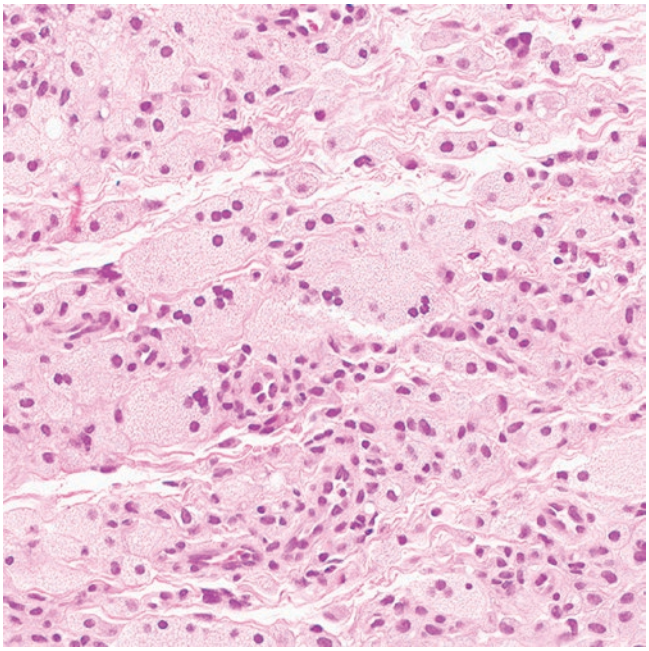

**Fig. 7.14** Tissue infiltration by large pale foamy histiocytes is the characteristic histopathological finding in Erdheim-Chester disease

a diagnosis of pulmonary ECD include interlobular septal and visceral pleural thickening, patchy reticular and centrilobular opacities, and ground glass attenuation (Fig. 7.13) [43]. The clinical course for patients with ECD is highly variable and can range from stable to rapidly progressive disease, especially in patients with systemic manifestations. Patients with pulmonary involvement have an overall 3-year survival of 66% [40]. Factors associated with poor prognosis are primarily neurologic and cardiac involvement [44, 45]. The treatment of patients with ECD has long consisted of corticosteroids or immunosuppressive agents until more recently interferon-based therapy has emerged as a reliable alternative [46, 47]. Inhibition of *BRAF* activation through *BRAF* inhibitors appears to be a promising new treatment in patients known to carry activating *BRAF* mutations and who have failed to respond to other types of treatment [41, 42].

### 7.2.2 Pathological Features

Low power magnification of lung wedge biopsies shows interstitial thickening with a lymphangitic distribution and expansion of the visceral pleura, interlobular septa, and bronchovascular bundles by a combination of fibrosis and inflammation [48, 49]. Closer examination will reveal that the fibrotic areas are infiltrated by a proliferation of large histiocytes with round to oval nuclei and pale staining foamy or finely granular cytoplasm (Fig. 7.14). The histiocytes are typically distributed in a single cell arrangement without distinct granuloma formation and lack the characteristic grooved nuclei that are typical for Langerhans cells. Aside from histiocytes, variable numbers of lymphocytes, plasma cells, and multinucleated Touton-type giant cells may also be noted. Emperipolesis is not a feature of ECD [48, 49].

### 7.2.3 Laboratory, Immunohistochemical, Ultrastructural, and Molecular Features

Bronchoalveolar lavage (BAL) fluid often has an opalescent appearance on gross examination; microscopic examination reveals the presence of abundant foamy histiocytes [46]. Immunohistochemically, the histiocytes of ECD express CD68 while S100 protein is more variable. In contrast to Langerhans cells, CD1a is negative in ECD (Table 7.2). Likewise, Birbeck granules are not identified on ultrastructural analysis [48, 49]. On a molecular level, *BRAF V600E* mutations have been identified in more than half of all cases of ECD and promising results have been reported with *BRAF* inhibitor treatment [41, 42].

### 7.2.4 Differential Diagnosis

Pulmonary involvement by ECD needs to be differentiated from other interstitial lung diseases and histiocytic disorders. Among the interstitial lung diseases usual interstitial pneumonitis (UIP) can show pleural and septal fibrosis, however, the temporal heterogeneity of UIP with alternating zones of fibroblastic foci, mature fibrosis and normal lung is not a feature of ECD. In ECD, the fibrosis is uniform and infiltrated by the characteristic histiocytic proliferation. Separation of ECD

from Langerhans cell histiocytosis requires close attention to the distribution and composition of the histiocytic proliferation. In Langerhans cell histiocytosis, histiocytic nodules are primarily seen in a peribronchiolar distribution, while in ECD, the infiltrate is mainly seen in an angiocentric and pleural pattern. Moreover, Langerhans cells have characteristic nuclear grooves and folds and indistinct cytoplasm, while the histiocytes in ECD demonstrate abundant foamy cytoplasm. Rarely, Rosai-Dorfman disease (RDD) has been reported in the lung. In most of these cases, the histiocytic infiltrate forms a tumor-like mass, however an interstitial pattern of involvement has also been reported which may be difficult to distinguish from ECD. Close attention to the cytologic features may identify the presence of lymphocytes or other inflammatory cells in the cytoplasm of RDD cells (emperipolesis). This phenomenon is not usually a feature of the histiocytes of ECD. Separation of ECD from other histiocytic disorders can also be accomplished by the use of immunohistochemical markers: while the histiocytes of ECD express CD68 and only occasionally S100, Langerhans cells are positive for S100, CD1a, and langerin, and the cells in RDD are consistently positive for S100 and CD68 but negative for CD1a [48, 49] (Table 7.2).

## 7.3 Rosai-Dorfman Disease

Rosai-Dorfman disease (RDD) also known as *sinus histiocytosis with massive lymphadenopathy* is a rare polyclonal histiocytic disorder that usually presents as painless cervical lymphadenopathy in individuals in the 1st or 2nd decade of life [50]. Extranodal disease has subsequently been recognized in many organ systems, most commonly in the head and neck area, skin, and soft tissues [51]. Intrathoracic involvement, although previously thought to be uncommon, can be seen in up to 43% of cases, mainly in the form of mediastinal lymphadenopathy [51, 52]. More rarely, RDD can present with lung masses mimicking lung cancer [53–58] or as an interstitial infiltrate mirroring interstitial lung disease [52, 59–61]. The etiology and pathogenesis of RDD are still uncertain although proposed causes include infection, an exaggerated immune response to an infectious or non-infectious antigens [2], or an autoimmune component [51]. More recently, elevated numbers of IgG4-positive plasma cells have been reported in a subset of RDD cases leading the authors to speculate that RDD and IgG4-related disease might overlap to some extent [54, 60, 62, 63]. On the other hand, other authors have argued against such a relationship due to an absence of other morphological similarities and numbers of IgG4-positive cells in RDD that were similar to reactive lymph nodes [64]. Contrary to other histiocytoses, activating mutations of the *BRAF* gene have not been identified in any of the cases of RDD mitigating against a role of this gene in the pathophysiology of the disease [41]. Therefore, the precise cause for RDD remains to be determined.

### 7.3.1 Clinical Features

Intrathoracic RDD affects patients of both sexes equally and over a wide age range. Contrary to Langerhans cell histiocytosis, there is no direct link to cigarette smoking. Dyspnea, cough, and chest pain are the primary symptoms although some patients may be asymptomatic. Spirometry can show normal, restrictive, or obstructive patterns [51]. Radiologic imaging will reveal well-circumscribed or spiculated masses in the lung parenchyma with or without associated hilar adenopathy [52–54, 56–58] or diffuse bilateral lung lesions with reticulation, consolidation, or infiltrates [52, 59–61]. Treatment for patients with pulmonary RDD consists of corticosteroids, interferon therapy, chemotherapy, and radiation therapy although the benefit of such therapies has not been fully proven [65]. Surgical management may become necessary when vital structures are compromised; however, postoperative recurrences have been described [55, 58, 66–69]. Although the prognosis for patients with lung involvement by RDD was initially thought to be guarded [51], more recent studies of patients with localized thoracic involvement have largely demonstrated a favorable outcome although longitudinal studies are lacking [53–55].

### 7.3.2 Pathological Features

On gross examination, pulmonary RDD shows relatively circumscribed masses with a yellow-white color and soft center [56]. Histologically, the lesions are composed of a diffuse infiltrate of large histiocytoid cells intermixed with lymphocytes, plasma cells, neutrophils, and eosinophils (Fig. 7.15a, b). The histiocytes have abundant cytoplasm, vesicular nuclei, and prominent nucleoli (Fig. 7.16). The hallmark feature of the histiocytes in RDD is emperipolesis, i.e., the engulfment of viable lymphocytes, plasma cells, neutrophils, or erythrocytes in the cytoplasm of these cells [50] (Fig. 7.17). Associated findings may include alveolar wall thickening, type II pneumocyte hyperplasia, and foamy cells in the alveolar spaces of the adjacent lung parenchyma. Peribronchial lymph node involvement may also be seen [54–57, 70]. In the interstitial form, the histiocytes and inflammatory cells are distributed in a perilymphatic pattern and can show variable degrees of fibrosis [52, 59–61]. Of note, in some cases, the plasma cells can express IgG4 and show elevated IgG4:IgG ratios as well as foci of obliterative phlebitis suggesting a degree of overlap with IgG4-related disease [54, 59, 60, 62]. Cases of tracheobronchial involvement with lesions located in the tracheobronchial wall are also well described [71].

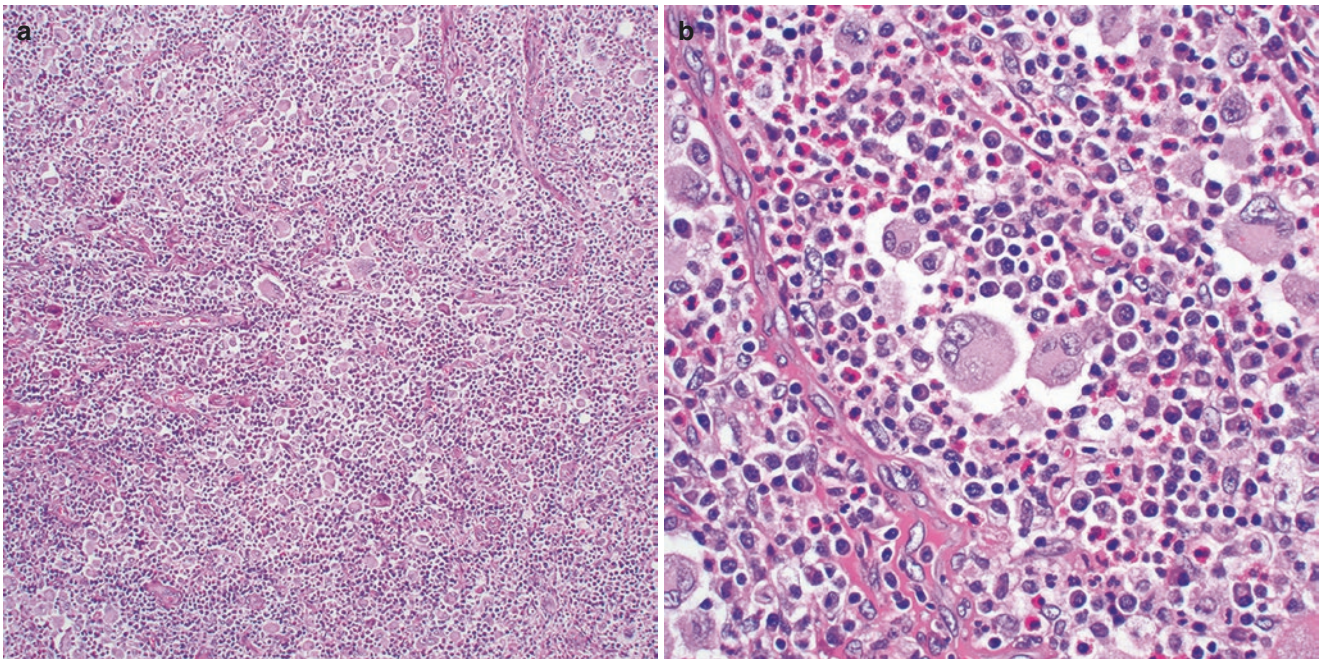


**Fig. 7.15** (**a**) Rosai-Dorfman disease composed of sheets of histiocytes and other inflammatory cells; (**b**) the cellular components consist of large histiocytes and variable numbers of lymphocytes, plasma cells, and eosinophils

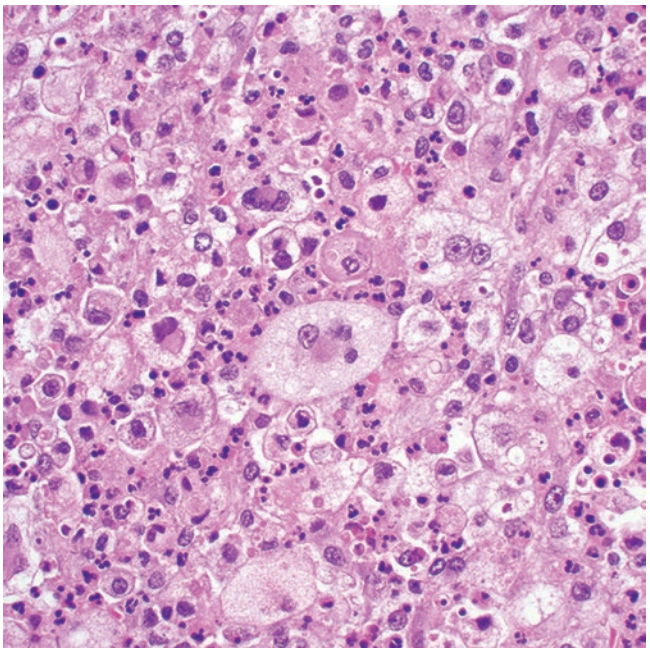

**Fig. 7.16** The histiocytes of Rosai-Dorfman disease have abundant cytoplasm, vesicular nuclei, and prominent nucleoli

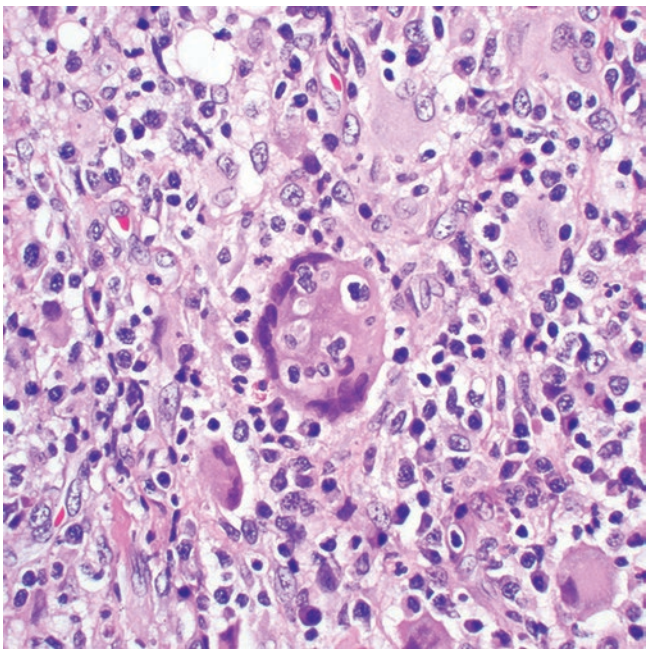

**Fig. 7.17** The hallmark of Rosai-Dorfman disease is emperipolesis, i.e., the presence of viable inflammatory cells in the cytoplasm of the histiocytes

### 7.3.3 Laboratory, Immunohistochemical, and Molecular Features

In some patients with RDD, laboratory investigations can reveal leukocytosis, anemia, elevated erythrocyte sedimentation rate, and polyclonal hypergammaglobulinemia [51]. Immunohistochemistry characteristically shows histiocytes that are strongly positive for S100 and CD68 while negative for CD1a [2] (Table 7.2) (Fig. 7.18). As opposed to Langerhans cell histiocytosis and Erdheim-Chester disease, activating *BRAF* or other recurring mutations have not been identified in RDD [41].

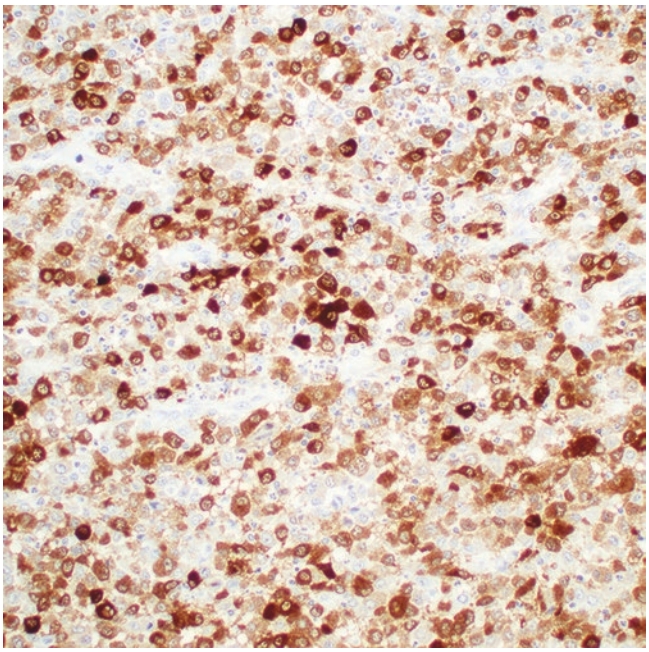

**Fig. 7.18** The histiocytes of Rosai-Dorfman disease typically strongly express S100 protein by immunohistochemistry

### 7.3.4 Differential Diagnosis

Langerhans cell histiocytosis and Erdheim-Chester disease on the one hand and fungal infections or metastatic malignancies on the other should be included in the differential diagnosis of pulmonary RDD. Langerhans cell histiocytosis and Erdheim-Chester disease may have similar disease distribution and cellular composition as RDD. However, in RDD, the characteristic histological finding is the presence of emperipolesis, which is absent in the other two disorders. In difficult cases, a panel of immunohistochemical markers, including S100, CD68, CD1a, and langerin, may help distinguish between the lesions (Table 7.2). In some instances, metastatic carcinoma or melanoma may be suspected. Contrary to the latter, metastatic malignancy will usually show prominent cytologic atypia which is not a feature of pulmonary RDD; in addition, carcinomas are characterized by an immunophenotype positive for cytokeratin, while melanomas, in addition to S100, will express other markers of melanocytic differentiation, including HMB45 or melan-A, markers that would be absent in the histiocytes of RDD.

## 7.4 Pulmonary Malakoplakia

Malakoplakia is a rare inflammatory condition characterized by the accumulation of histiocytes that can mimic the presence of a tumor mass [72]. Despite its first descriptions by Michaelis and Gutman in 1902 and von Hansemann in 1903 [73, 74], the pathogenesis of malakoplakia remains a matter of controversy. The literature suggests that malakoplakia develops due to defective lysosomal activity in response to bacterial infection leading to impairment of the normal phagocytic process and resulting in an abnormal intracellular digestion of bacteria [75]. Most cases of malakoplakia occur in the genitourinary tract and are associated with long-standing *Escherichia coli* infection. Pulmonary malakoplakia on the other hand is a very rare condition with only 40 reported cases in the medical literature [76–78]. Contrary to the urinary tract, in the pulmonary system, *Rhodococcus equi*, a gram-positive coccobacillus, is the most common pathogen that is linked with the disease [72].

### 7.4.1 Clinical Features

Malakoplakia is mainly seen in immunocompromised hosts such as patients with hematologic malignancies, organ transplant recipients, patients with acquired immunodeficiency syndrome (AIDS), or individuals on corticosteroid therapy [72]. Rarely, immunocompetent patients are affected. The disease usually has a subacute or chronic clinical course, and patients present with fever or other non-specific symptoms. Radiologic imaging can reveal solitary masses closely resembling primary lung malignancy, pneumonias with cavitation, or multiple pulmonary nodules. Tracheal or pleural involvement may also be seen [72, 77]. Of note, positron emission tomography (PET) may show increased fluorodeoxyglucose (FDG) uptake in pulmonary malakoplakia which can further increase the suspicion for a neoplastic process [72, 77]. Conservative treatment with antibiotics results in the regression of the disease in most cases; hence, correct diagnosis is important in order to avoid radical surgical intervention [77, 78].

### 7.4.2 Pathological Features

In pulmonary malakoplakia, the lung parenchyma is replaced by sheets of large histiocytes (von Hansemann cells) with foamy or eosinophilic granular cytoplasm and round eccentrically placed nuclei (Fig. 7.19a, b). Foci of necrosis and abscess formation can be present. Clusters of neutrophils, lymphocytes, and plasma cells may be admixed. The coccobacilli can often be demonstrated within the cytoplasm of the histiocytes using special stains. A characteristic finding is the presence of intracellular or extracellular target-shaped, concentric, laminated bodies containing bacterial remnants covered by iron and calcium deposits, the Michaelis-Gutmann bodies are commonly seen in malakoplakia and are considered pathognomonic for the disease [72, 76] (Fig. 7.20).

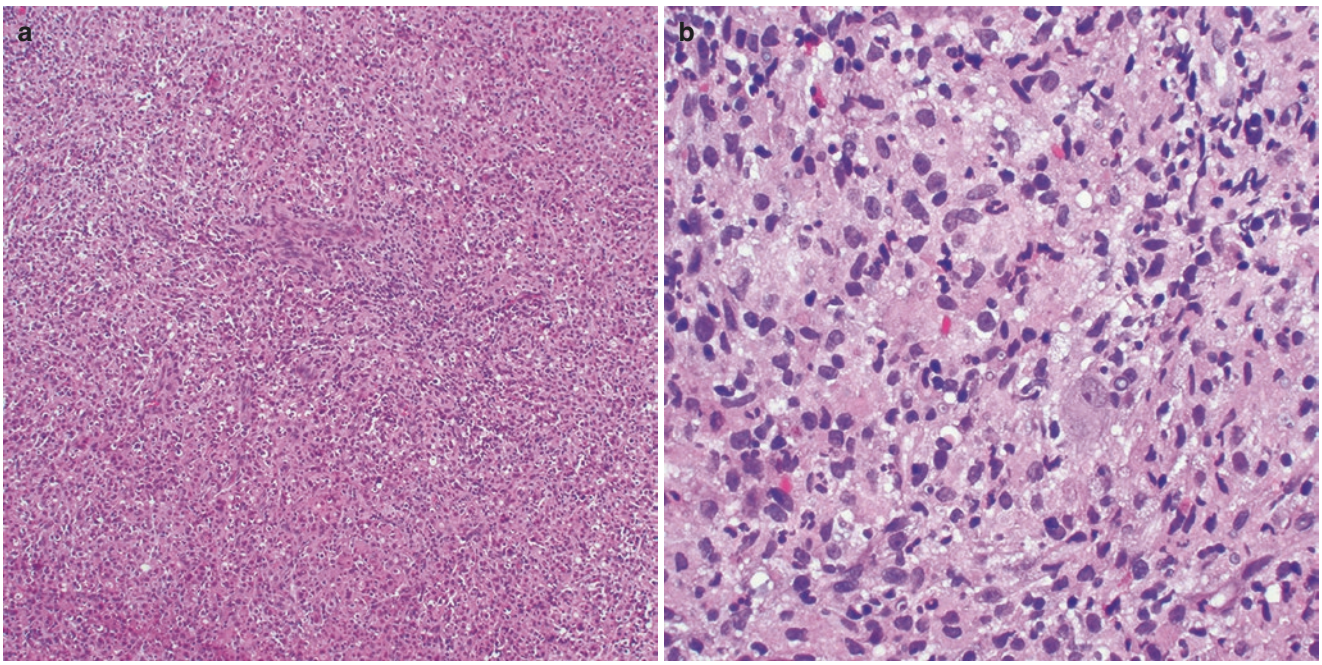


**Fig. 7.19** (**a**) Low power view of a case of malakoplakia showing sheets of histiocytes; (**b**) higher magnification shows that the histiocytes are large and contain ample cytoplasm

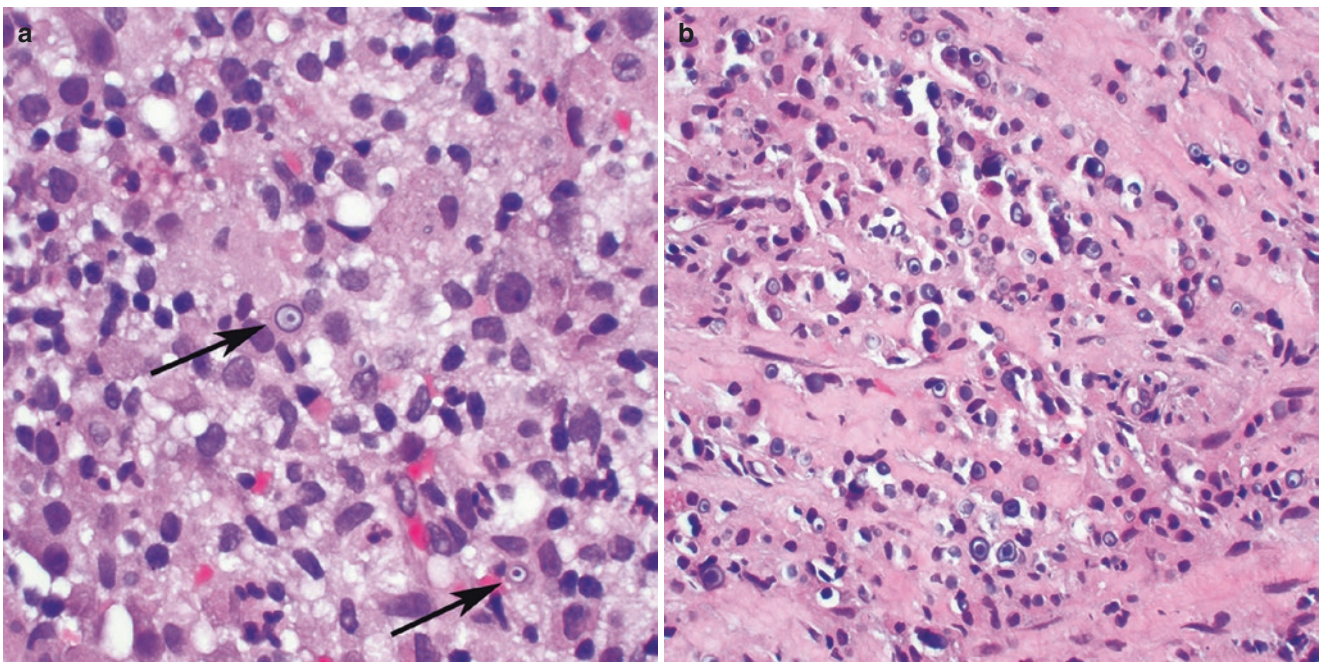


**Fig. 7.20** (**a**) Close scrutiny of the material will reveal the presence of characteristic Michaelis-Gutmann bodies with targetoid appearance (arrows) in pulmonary malakoplakia; (**b**) another case showing more abundant Michaelis-Gutmann bodies

### 7.4.3 Laboratory Diagnosis and Histochemical Stains

The organism can be isolated from sputum, blood, or lung tissue cultures. In tissue sections, the coccobacilli can be visualized using Gram, Gomori methenamine silver, or Grocott stains. Despite being weakly acid fast, identification of *Rhodococcus equi* using acid-fast or modified acid-fast stains is often unsuccessful [79, 80]. A polymerase chain reaction (PCR) assay is another rapid and highly sensitive method to detect the organism in tissue sections [78]. The cytoplasm of infected histiocytes can be intensely periodic

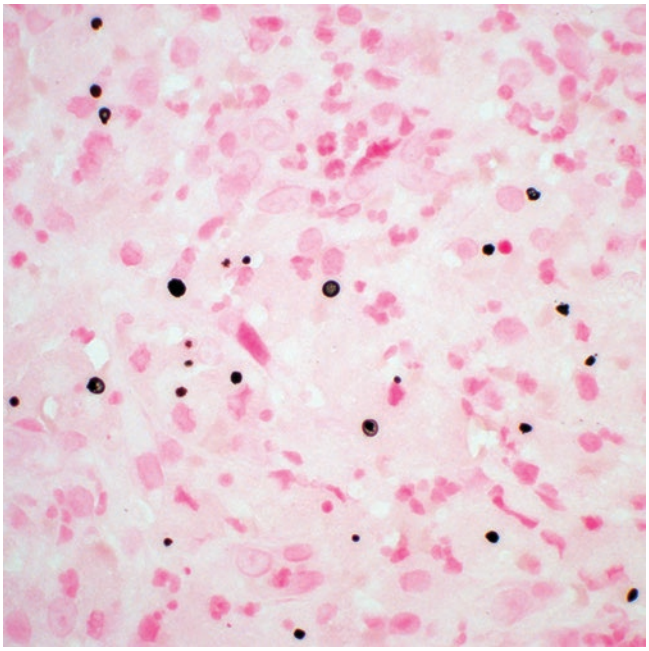

**Fig. 7.21** The Michaelis-Gutmann bodies of malakoplakia can be highlighted with a von Kossa histochemical stain

acid-Schiff (PAS)-positive often mimicking other diseases, such as Whipple disease [80]. Michaelis-Gutmann bodies can be highlighted with von Kossa, Giemsa, or iron special stains [79] (Fig. 7.21).

### 7.4.4 Differential Diagnosis

Pulmonary malakoplakia has the potential to be mistaken for other histiocytic disease processes as well as primary bronchogenic carcinomas. Identification of the characteristic Michaelis-Gutmann bodies will help distinguish malakoplakia from other conditions associated with a histiocytic infiltrate, while attention to the cytologic features of the infiltrate, such as absence of cytological atypia or mitotic activity, should exclude a neoplastic process. If still in doubt, immunohistochemical studies may be used to confirm the histiocytic origin in malakoplakia (CD68+, vimentin+) versus epithelial differentiation (pancytokeratin+) in primary lung carcinomas.

## 7.5 Pulmonary Whipple Disease

Whipple disease is a chronic systemic infection caused by *Tropheryma whipplei*, a ubiquitous commensal actinomycete that is present in up to 7% of healthy individuals [81–83]. Despite this, Whipple disease is a rare disorder with an incidence of around 0.5–1 case per million of the population, suggesting a role for immunogenic host susceptibility to the disease [84]. The classic form of the disease has a prodromal stage characterized by recurrent arthritis followed several years later by weight loss and diarrhea [85]. Thoracic involvement has been estimated to occur in 30–40% of cases, mostly in the form of hilar lymphadenopathy and pleural effusion; lung parenchymal disease is uncommon [86]. Typically, pulmonary involvement occurs late in the course of the disease and rarely at the time of presentation. Clinically, pulmonary Whipple disease can present in variety of different patterns, including interstitial lung disease, parenchymal nodules, or endobronchial lesions [86–89].

### 7.5.1 Clinical Features

Whipple disease can affect persons of all ages and races; however, it is most commonly seen in middle-age white men [85, 86]. Symptoms indicative of lung involvement most commonly include shortness of breath, dry cough, and chest pain [86]. Arthralgias, migratory arthritis, intermittent fever, weight loss, and diarrhea often precede the onset of respiratory disease [86, 87, 90]. Radiologic abnormalities include nodular or reticulonodular interstitial patterns or pulmonary nodules and masses mimicking neoplastic disease [86, 87]. Clinical improvement is usually rapid with antibiotic treatment; however, recurrence is not uncommon, especially in patients with central nervous system involvement. Untreated Whipple disease remains a potentially fatal condition [91].

### 7.5.2 Pathological Features

Examination of tissue specimens from endobronchial or wedge biopsies of the lung show a characteristic infiltrate of voluminous histiocytes with foamy cytoplasm that often cluster in aggregates and that can present in a variety of different patterns, including interstitial distribution along the lymphatic/peribronchiolar routes or as intraalveolar accumulations (Fig. 7.22). Concurrent findings can include non-caseating granulomatous inflammation mimicking sarcoidosis or an acute fibrinous and organizing pneumonia (AFOP) pattern [86, 92].

### 7.5.3 Laboratory Diagnosis, Histochemical, and Immunohistochemical Stains

*Tropheryma whipplei* is a Gram-positive rod-shaped bacillus that contrary to mycobacteria is not acid fast. The organisms can be highlighted in the cytoplasm of the histiocytes with a periodic acid-Schiff (PAS) stain where they form characteristic globular inclusions [93] (Fig. 7.23) or with specific immunohistochemical antibodies [91]. The most sensitive diagnostic test, however, is identification of the organism using polymerase chain reaction (PCR) methods in stool, saliva, or frozen tissue sections from involved organ sites [86].

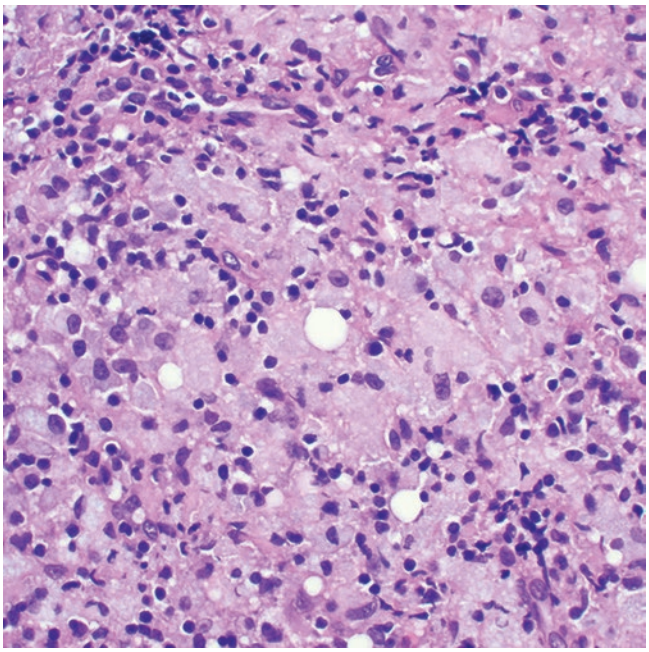

**Fig. 7.22** Sheets of pale staining histiocytes are the characteristic finding in pulmonary Whipple disease

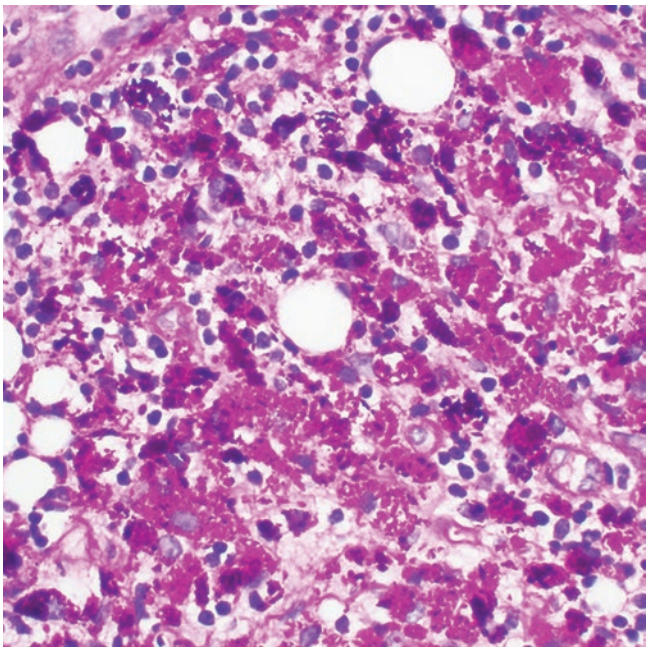

**Fig. 7.23** A periodic acid-Schiff stain highlights the cytoplasmic globular inclusions in Whipple disease

### 7.5.4 Differential Diagnosis

Due to the varying patterns of the disease in the lung parenchyma, the histopathological differential diagnosis can include a wide range of other conditions; however, based on the presence of foamy macrophages and/or non-caseating granulomas, mycobacterial infection and sarcoidosis need to be excluded in the first instance. In addition to the presence of foamy macrophages, mycobacterial infections often present with necrotizing granulomatous lesions, unlike Whipple disease. Although in both cases rod-shaped bacilli can be identified, in Whipple disease, the organisms are PAS-positive and not acid fast, while in mycobacterial infections the opposite is true. In cases of doubt, PCR or culture studies may help identify the causative agent. Sarcoidosis may enter the differential diagnosis based on the presence of non-necrotizing granulomas. However, in sarcoidosis, the characteristic infiltrate of foamy histiocytes of Whipple disease is uncommon, and microorganisms are absent. Close attention to the clinical pattern of presentation may be of further aid in the differential diagnosis.

## 7.6 Crystal-Storing Histiocytosis

Crystal-storing histiocytosis (CSH) is a rare localized or systemic disorder characterized by an accumulation of large histiocytes with intracytoplasmic refractile eosinophilic crystals [94, 95]. As many of 90% of patients with CSH have an underlying lymphoproliferative disorder or plasma cell disease, including multiple myeloma, isolated plasma cell tumors, monoclonal gammopathy, lymphoplasmacytic lymphoma, or mucosa-associated lymphoid tissue (MALT) lymphoma [96]. Occasionally, CSH can present as a reactive process associated with immunologic defects, such as rheumatoid arthritis or Crohn's disease [96]. In the systemic form, two or more organ sites are involved, typically the bone marrow and other extramedullary sites and only rarely the lungs [97]. On the other hand, the lungs are the second most common site after the head and neck region for the localized form of CSH [96]. The precise etiology of CSH remains unknown, but overproduction of immunoglobulins with subsequent ingestion by histiocytes or abnormal secretion of immunoglobulins due to defects in intralysosomal degradation has been suggested [95, 96, 98]. The importance of the recognition of CSH lies in the fact that the vast majority of cases are associated with lymphoproliferative disorders requiring careful clinical workup to rule out such possibility.

### 7.6.1 Clinical Features

Patients with pleuropulmonary CSH are typically older individuals with a mean age at diagnosis in the 7th decade of life [99]. Many patients are asymptomatic, and their disease is discovered incidentally. Presenting symptoms may include dyspnea, chest pain, or fever. Radiologically, CSH presents as pleural or pulmonary nodules and masses with or without cystic changes and calcifications [99]. CSH in

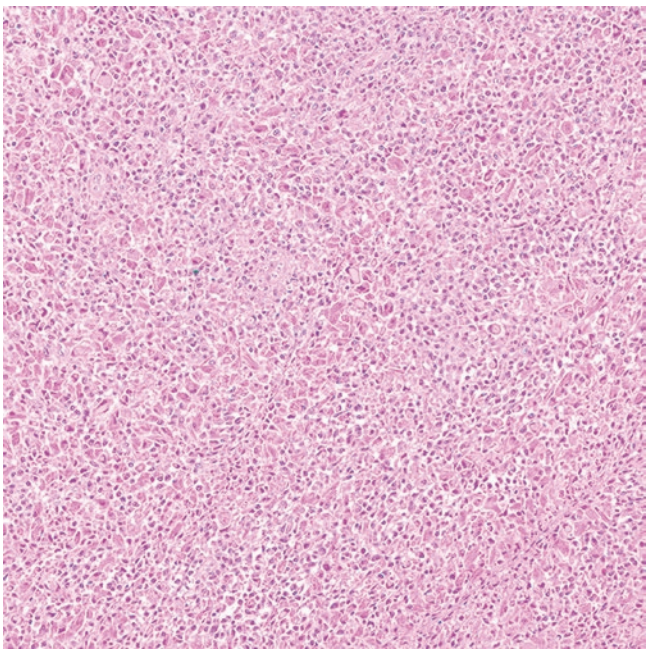

**Fig. 7.24** Crystal-storing histiocytosis is characterized by sheets of large polygonal histiocytes

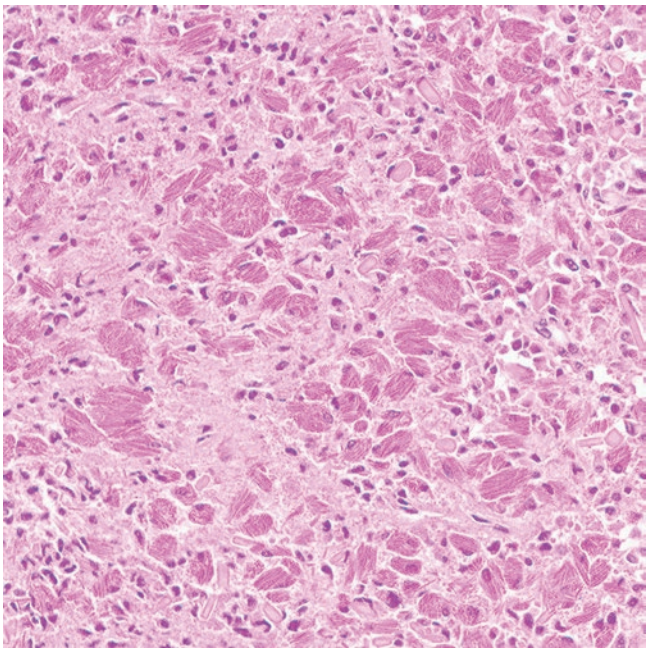

**Fig. 7.25** Higher magnification shows abundant striated crystalline inclusions in the cytoplasm of the histiocytes in crystal-storing histiocytosis

the context of systemic lymphoproliferative disease is often associated with a poor prognosis, regardless of the type of neoplasm [100]. In contrast, the biologic behavior of patients with localized CSH is more variable and in the lung usually follows an indolent, non-progressive clinical course [101, 102].

### 7.6.2 Pathological Features

Grossly, the lesions of CSH show well-circumscribed but unencapsulated masses with a white cut surface [102]. Low power histological examination will show sheets of large polygonal histiocytes with voluminous eosinophilic cytoplasm replacing the lung parenchyma (Fig. 7.24). Higher magnification will reveal that the cytoplasm is filled with variably refractile and striated crystalline inclusions (Fig. 7.25). The small, bland nuclei are often pushed to the periphery of the cells. Mitotic activity is typically absent, but foci of coagulative necrosis may be observed. In the periphery of lesions, the process can infiltrate into alveolar septa, interlobular septa, and bronchovascular bundles and can cause a desquamative interstitial pneumonitis (DIP)-like reaction in adjacent alveolar spaces [102–105]. Other common findings include nodular aggregates of monocytoid lymphocytes in cases associated with MALT lymphoma and variable lymphoid or plasma cell infiltrates in cases with concurrent lymphoproliferative or plasma cell disorders [99]. In the latter, similar crystalline inclusions can be found in the cytoplasm of the neoplastic plasma cells [102].

### 7.6.3 Histochemical, Immunohistochemical, and Ultrastructural Features

The diagnosis of CSH rests on the identification of the characteristic crystalline inclusions in the cytoplasm of the histiocytes. The histiocytic nature of the lesional cells can be confirmed immunohistochemically by a positive reaction with CD68, while S100 and CD1a are negative. The inclusions are typically negative with a periodic acid-Schiff (PAS) histochemical stain but are strongly immunoreactive with various immunoglobulins as well as kappa light chains in the majority of cases (Fig. 7.26). Ultrastructural studies demonstrate electron-dense, membrane-bound, rhomboid, and needle-shaped intracytoplasmic crystals [100–103].

### 7.6.4 Differential Diagnosis

The differential diagnosis of CSH includes several other entities that present as histiocyte-rich lesions in the lung. Infections with prominent histiocytic appearance (mycobacterial infection, Whipple disease, and malakoplakia), storage diseases, and certain neoplasms can closely mimic pulmonary CSH. Mycobacterial infection can present with a prominent histiocytic infiltrate but lacks the characteristic cytoplasmic inclusions of CSH. On the other hand, Whipple disease is characterized by cytoplasmic inclusions; however, these consist of accumulations of the causative organism rather than the crystalline inclusions of CSH. In malakoplakia, the histiocytes

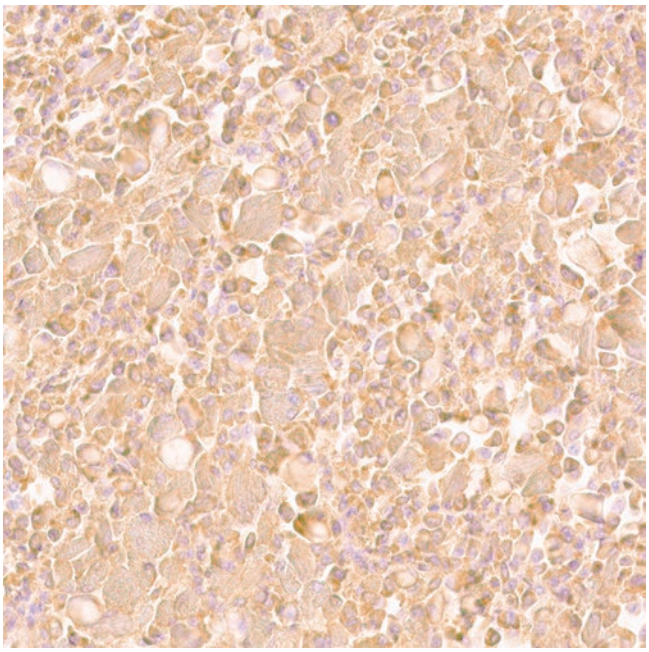

**Fig. 7.26** Expression of IgG by immunohistochemistry in a case of crystal-storing histiocytosis

contain laminated Michaelis-Gutmann bodies that are easily separated from the needle-shaped striated crystals in CSH. Histochemical stains such as PAS, acid-fast bacilli (AFB), and von Kossa stains can be used to separate these lesions in difficult cases. Among the storage diseases, Gaucher disease can closely resemble CSH. Gaucher disease, however, is more infiltrative in nature and not usually known to form mass lesions. In addition, Gaucher cells contain pale-staining striated inclusions that are strongly positive with iron stains as opposed to the tinctorial and refractile properties of the inclusions in CSH. Within the spectrum of neoplastic disease, granular cell tumors can occasionally occur in the lungs. Their tumor cells have a prominent histiocytic appearance containing bland nuclei and abundant granular cytoplasm; contrary to CSH, granular cell tumors do not contain any cytoplasmic inclusions and show strong and diffuse expression of S100 protein facilitating separation of the two conditions.

## 7.7 Pulmonary Storage Diseases

Storage diseases, such as Gaucher disease, Niemann-Pick disease, and Fabry disease, can also involve the lungs [106–108]. They belong to a group of familial lysosomal storage disorders that are caused by defects in lysosomal enzyme function and lead to accumulation of storage material in phagocytic cells of the monocyte-macrophage lineage throughout the body (Table 7.3). Histologically, this is reflected in the presence of abundant foamy macrophages containing glucocerebroside (Gaucher disease), sphingomyelin (Niemann-Pick disease), or glycosphingolipids (Fabry disease). Presentation with pulmonary disease is very uncommon as the diagnosis of storage disorders is usually made on the basis of extrapulmonary disease. In occasional cases, however, lung disease can be the primary presentation and lead to eventual diagnosis of an underlying storage disorder [107, 109, 110].

### 7.7.1 Clinical Features

Lung-related symptoms in storage disorders include dyspnea, wheezing, cough, and hemoptysis, or patients may be entirely asymptomatic [111]. Radiologically, storage diseases can present with interlobular septal thickening and ground glass opacities with or without crazy-paving and mosaic attenuation patterns [43]. Enzyme replacement and substrate reduction therapy have been successfully used in patients with Gaucher and Fabry disease, while whole-lung lavage and hematopoietic stem cell transplantation are current treatment strategies for Niemann-Pick disease [107, 112–114].

### 7.7.2 Pathological Features

Histological sections of the lungs in *Gaucher disease* will typically show infiltration by groups of lipid-laden macrophages (*Gaucher cells*) that can have round, spindled, or polygonal shapes and that often demonstrate apparent cohesion. These cells can involve the lung in various different patterns: (a) as patchy interstitial infiltrates corresponding to the distribution of lymphatics; (b) as accumulation of cells in the peribronchial and perivascular spaces and in the alveolar septa causing massive thickening thereof; (c) as infiltrates within septal capillaries with the potential to cause pulmonary hypertension and cor pulmonale; and (d) filling the alveoli in a pattern reminiscent of desquamative interstitial pneumonia (DIP) [106]. Higher magnification of the Gaucher cells shows an abundant pink cytoplasm with fine linear striations resembling crumpled tissue paper and absence of stainable iron [106]. In Niemann-Pick disease, the lung architecture is generally preserved. The main histological feature is accumulation of lipid-laden macrophages (*Niemann-Pick cells*) in the alveolar spaces, causing a type of endogenous lipoid pneumonia (Fig. 7.27a, b). Niemann-Pick cells can also infiltrate the interstitium, subpleural spaces (Fig. 7.28), and lymphatics, however without any apparent architectural distortion, fibrosis, or inflammation [44, 106, 115]. High power examination of Niemann-Pick cells shows histiocytes with abundant finely vacuolated foamy cytoplasm containing granular material [44, 106, 115] (Fig. 7.29). In Fabry disease, lamellar inclusion bodies are found in respiratory epithelial cells, endothelial cells, and bronchial and vascular smooth muscle cells commonly leading to airway obstruction [108].

**Table 7.3** Key features of pulmonary storage diseases

| | Gaucher disease | Niemann-Pick disease | Fabry disease |
|---|---|---|---|
| Inheritance pattern | Autosomal recessive | Autosomal recessive | X-linked |
| Mutations | *β-Glucocerebrosidase* gene | *Sphingomyelin phosphodiesterase 1 (SMPD1)* gene (types A and B); *Niemann-Pick disease, type C1 (NPC1) and type C2 (NPC2)* genes (type C) | *α-Galactosidase* mutation |
| Deficient enzyme | Glucocerebrosidase | Acid sphingomyelinase | α-Galactosidase A |
| Clinical subtypes | *Type I (non-neuropathic):* early life or adulthood, severe; no CNS involvement<br>*Type II (acute infantile neuropathic):* within first 6 months of life; extensive CNS damage; lethal<br>*Type III (chronic neuropathic):* childhood or adulthood; slowly progressive CNS symptoms | *Type A:* absence of acid sphingomyelinase; severe neurodegeneration and death in early childhood<br>*Type B:* deficiency of acid sphingomyelinase; little or no neurologic disease with survival into adulthood<br>*Type C:* deficiency of lipid transportation; progressive neurologic dysfunction | – |
| Systemic manifestations | Organomegaly (liver, spleen) and hematologic dysfunction, variable neurologic symptoms | Organomegaly (liver, spleen) and hematologic dysfunction, variable neurologic symptoms | Acroparesthesias; cutaneous angiokeratomas; progressive renal disease and cardiac involvement |
| Pulmonary manifestations | Infiltration of alveolar walls, alveolar spaces and alveolar septal capillaries by Gaucher cells | Endogenous lipoid pneumonia due to accumulation of Niemann-Pick cells in alveolar spaces | Small airway disease due to accumulation of inclusion bodies in respiratory epithelial cells and smooth muscle cells of airways and vasculature |
| Primary cell type | *Gaucher cell:* Lipid-laden macrophages with crumpled tissue paper appearance | *Niemann-Pick cell:* Large granular macrophages; "sea blue histiocytes" on May-Grünwald-Giemsa stain | – |
| Treatment | Enzyme replacement, substrate reduction therapies | Whole-lung lavage, hematopoietic stem cell transplantation | Enzyme replacement |

*CNS* central nervous system

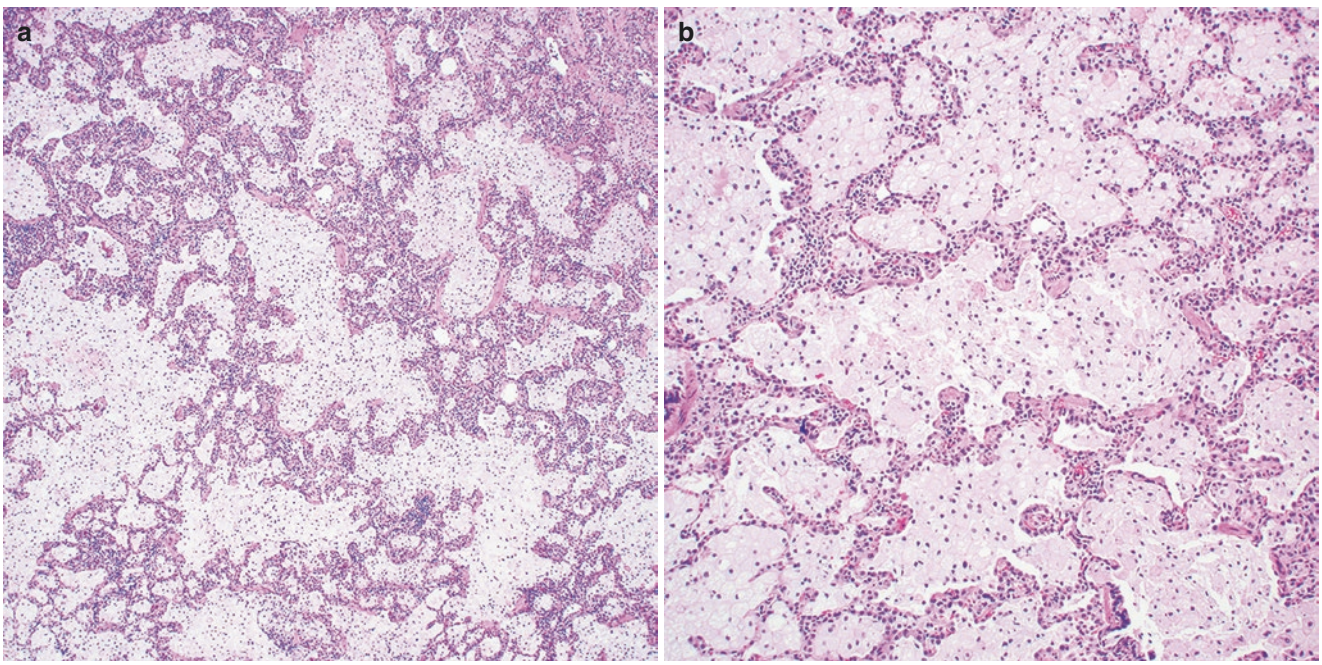


**Fig. 7.27** (**a**) Pulmonary Niemann-Pick disease with endogenous lipoid pneumonia; (**b**) higher power view shows a diffuse accumulation of histiocytes within the alveolar spaces. (Courtesy of Dr. A Al-Ibraheemi, Boston, USA)

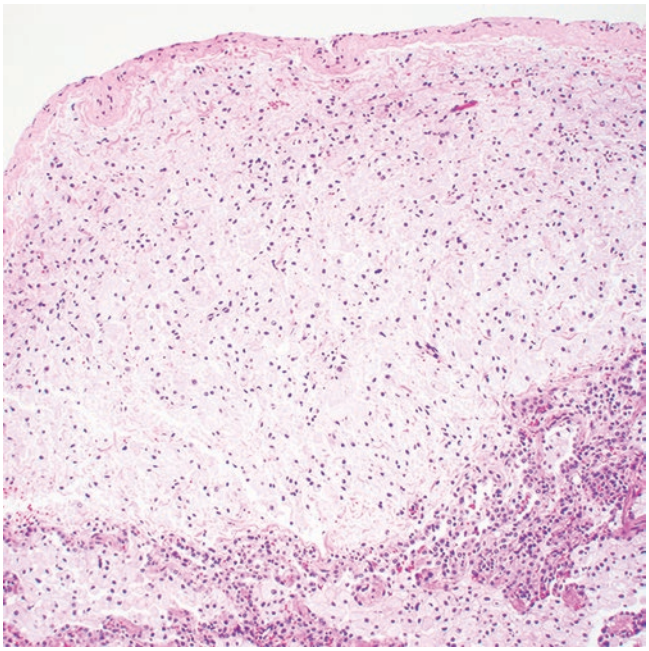

**Fig. 7.28** Collections of Niemann-Pick cells can also be seen in a subpleural fashion. (Courtesy of Dr. A Al-Ibraheemi, Boston, USA)

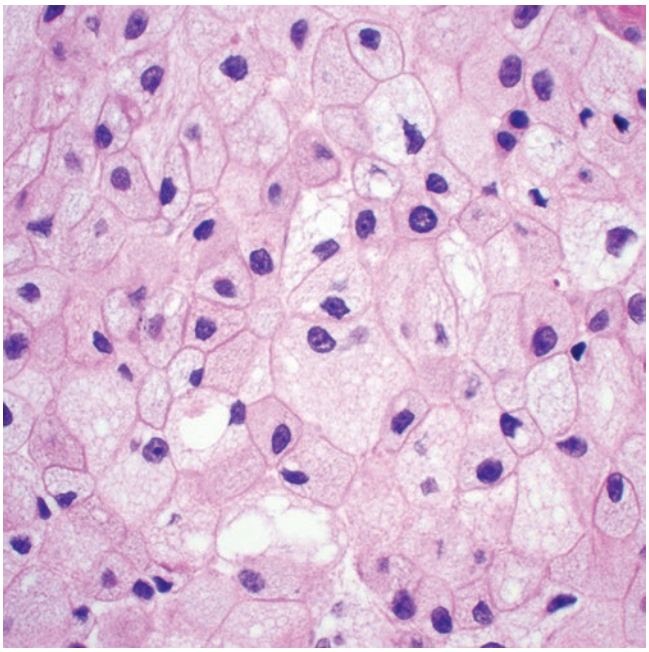

**Fig. 7.29** High power view of the cells in Niemann-Pick disease shows histiocytes with abundant foamy or granular cytoplasm. (Courtesy of Dr. A Al-Ibraheemi, Boston, USA)

### 7.7.3 Histochemical, Immunohistochemical, and Ultrastructural Features

The histiocytic origin of the cells in storage disorders is substantiated with a CD68 immunostain. Other characteristic staining patterns include a prominent pink appearance of

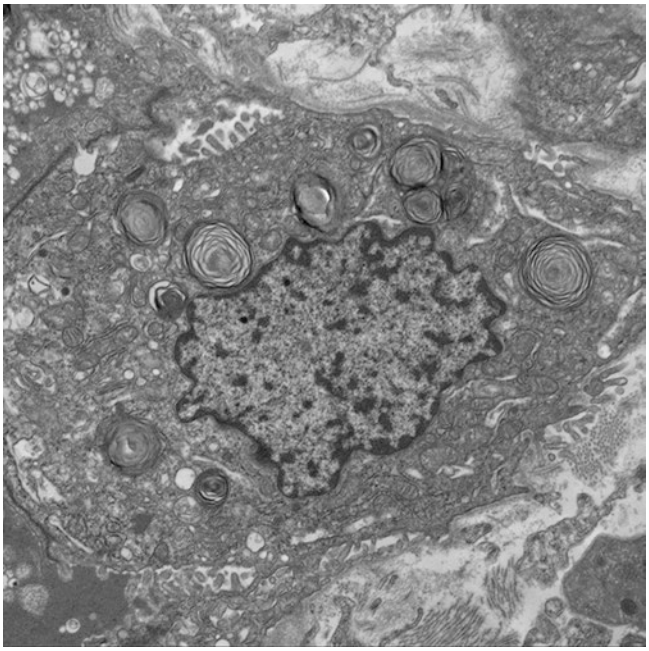

**Fig. 7.30** Electron microscopy of a Niemann-Pick cell showing a histiocyte containing abundant lysosomes filled with lamellar material. (Courtesy of Dr. A Al-Ibraheemi, Boston, USA)

Gaucher cells on conventional hematoxylin-eosin stains and deep blue quality (*sea-blue histiocytes*) of the granular histiocytes of Niemann-Pick disease with a May-Grünwald-Giemsa stain. Ultrastructural techniques show accumulation of lysosomes in the cytoplasm of the phagocytic cells. The lysosomal structures are typically elongated and distended and filled with irregular lamellar or tubular material [107, 108] (Fig. 7.30).

### 7.7.4 Differential Diagnosis

The histological differential diagnosis for patients with storage diseases includes a wide range of different disorders, including native alveolar macrophage accumulation, a DIP-like reaction, endogenous lipoid pneumonias of other causes, and drug toxicity. Reactive macrophages are generally smaller, rounder, and less cohesive than the lipid-filled histiocytes of Gaucher or Niemann-Pick disease. In addition, alveolar macrophages often lack the striated or granular properties of these cells and often contain hemosiderin which can be highlighted with iron stains. The same is true for DIP-like reactions that basically consist of collections of reactive alveolar macrophages in the alveolar spaces, either in primary DIP or as a secondary phenomenon due to various pulmonary disorders. An endogenous lipoid pneumonia similar to the pulmonary manifestations of Niemann-Pick disease is commonly seen as a reactive pattern to airway obstruction, for instance, due to tumors, or in relation to inflammation

and repair. In these situations, however, the foci of endogenous lipoid pneumonia are usually restricted to the area affected and do not diffusely involve the lung as in Niemann-Pick disease. Diffuse involvement of the lung by an endogenous lipoid pneumonia on the other hand can be seen as a reaction to drug therapy, more specifically amiodarone toxicity. Although the latter often shows foamy changes, the histological feature of amiodarone toxicity lacks the degree of interstitial and septal infiltration that can be seen in storage disease.

## 7.8 Pulmonary Xanthomatous Lesions

Pulmonary xanthomatous proliferations include xanthomas and pulmonary juvenile xanthogranulomas (PJXG). These are rare benign lesions in the lung that typically affect children and young adults [116–119]. Although multiple reports have been published describing xanthomatous tumors arising in the lung, from the descriptions and photographs, it appears that most of these likely exemplify what are today considered inflammatory pseudotumors (IPT) of the lung [120–124]. In this context, only one publication seems to represent a true pulmonary xanthoma [116]. Juvenile xanthogranulomas are benign cutaneous lesions of childhood that often involute spontaneously. They belong to the non-Langerhans cell histiocytic proliferative disorders of unknown pathogenesis although origin from dermal dendritic cells or plasmacytoid monocytes has been proposed [125]. Though predominantly a cutaneous disease, systemic involvement has been described in up to 5% of cases, and many organ systems, including the bronchopulmonary system, may be affected [126].

### 7.8.1 Clinical Features

Pulmonary xanthomas and PJXG primarily affect children and young adults many of whom have a history of lipoprotein disorders (xanthoma) or coexisting cutaneous or other visceral lesions (xanthoma and PJXP). Rarely, the lung lesion may be the only manifestation of the disease, which can make the diagnostic process extremely challenging. Cough, dyspnea, hemoptysis, and chest pain are the most common presenting symptoms although the lesions may also be incidental findings during the workup for lesions in other organ sites [116–119]. On radiologic imaging, the lesions most often manifest as well-circumscribed solitary or multiple bilateral round nodules or masses or more rarely as micronodular interstitial lesions [116–119]. Of note, positron emission tomography can demonstrate high [$^{18}$F]-2-fluoro-2-deoxy-D-glucose (FDG) uptake closely mimicking a malignant process [119]. Although most cutaneous lesions generally involute spontaneously, surgical excision is typically performed for their pulmonary analogues, usually because of functional impairment or diagnostic uncertainty [116–119].

### 7.8.2 Pathological Features

The only reported pulmonary xanthoma was described as a large well-circumscribed lesion in the lung parenchyma which was surrounded by a membranous capsule and which had a yellow cut surface without obvious hemorrhage or necrosis. Histological sections revealed a homogeneous proliferation of large histiocytic cells with abundant foamy cytoplasm and bland cytologic features and without any evidence of hemorrhage, necrosis, or mitotic activity [116] (Fig. 7.31a–c). Likewise, PJXG are well-demarcated but unencapsulated micronodules or masses with a cream or yellow color and soft consistency. Histologically, PJXG show a proliferation of small- to medium-sized histiocytes with or without visible nucleoli, intermixed with lymphocytes and plasma cells and occasional Touton-like giant cells (Fig. 7.32a, b). Malignant cytologic features, prominent mitotic activity, and necrosis are typically absent [117–119].

### 7.8.3 Immunohistochemical and Ultrastructural Features

The histiocytic cells of both conditions have an immunophenotype characterized by reactivity for CD68 and factor XIIIa and negative staining for S100 protein, CD1a, and langerin (Fig. 7.33). Variable reactivity can be seen with leucocyte common antigen [117–119]. Contrary to Langerhans cell histiocytosis (LCH), the ultrastructural features of the lesional cells demonstrate bland fibrohistiocytic and/or xanthoma cells without any Birbeck granules although, in some cases, non-specific intracytoplasmic dense bodies, worm-like bodies, or popcorn bodies may be found [127].

### 7.8.4 Differential Diagnosis

The main differential diagnosis for both conditions is pulmonary IPT. IPT occurs in the lungs of young adults and has histological features that are very similar to the pulmonary xanthomatous lesions. They consist of a mixture of bland fibrohistiocytic spindle cells arranged in fascicles or storiform patterns mixed with inflammatory cells, including lymphocytes, plasma cells, and foamy histiocytes. All

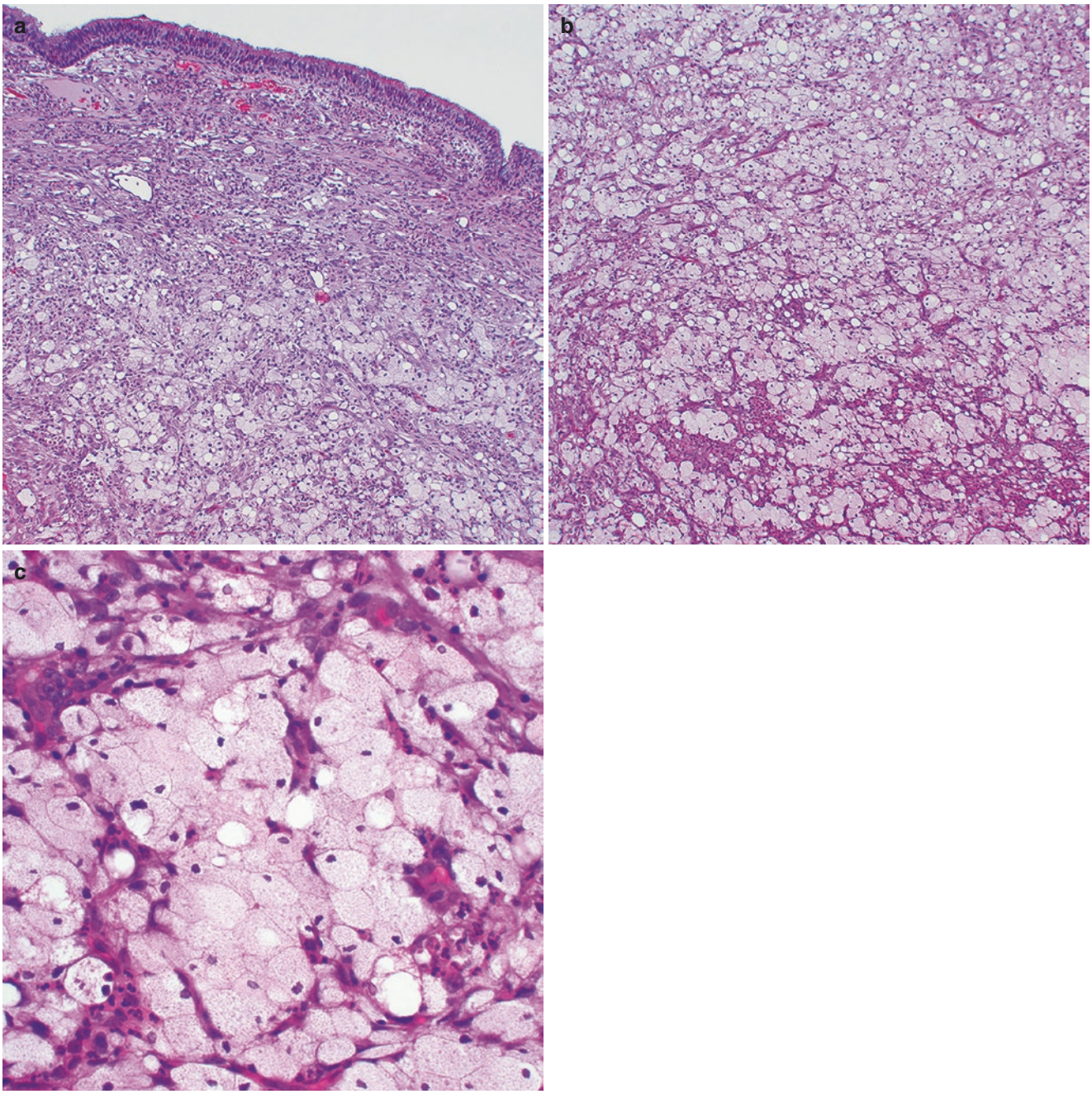


**Fig. 7.31** (**a**) Endobronchial xanthoma shows an accumulation of large histiocytes underneath the bronchial epithelium; (**b**) sheets and clusters of pale histiocytes in pulmonary xanthoma; (**c**) the histiocytes have abundant pale foamy cytoplasm and bland cytologic features

three lesions can display common immunoreactivity including expression of histiocytic markers and vimentin. In pulmonary xanthoma, however, there will be a very homogeneous proliferation of foamy xanthoma cells with a limited inflammatory cell infiltrate and lack of a spindle cell component. Likewise, a prominent fibroblastic/myofibroblastic proliferation is not a feature of PJXG. In addition, smooth muscle actin, a marker strongly associated with IPT, is usually negative in the xanthomatous lesions. Another common histiocytic disorder in children is LCH. LCH is typically a multifocal process consisting of parenchymal nodules composed of Langerhans cells with characteristic folded or grooved nuclei and varying numbers of eosinophils. Although the clinical presentation and histological features are usually distinct enough to distinguish LCH from the xanthomatous lesions, immunohistochemical studies can help separate these entities. Classically, the histiocytes of LCH express S100 protein, CD1a, and langerin, while xanthomatous histiocytes are limited to expression of CD68 and factor XIII. Furthermore, electron microscopy will reveal Birbeck granules in LCH but not in the xanthomatous cells.

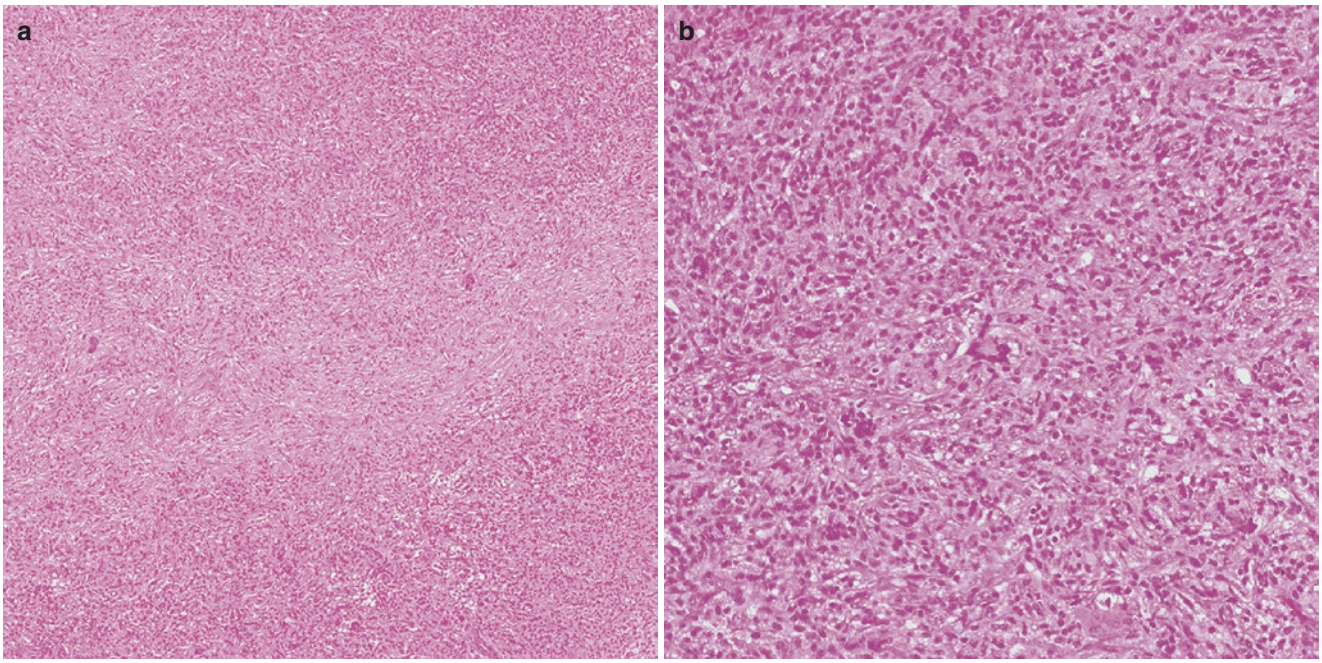


**Fig. 7.32** (**a**) Juvenile xanthogranuloma shows a diffuse proliferation of histiocytes intermixed with other inflammatory cells; (**b**) occasional Touton-type giant cells are another typical finding in this condition

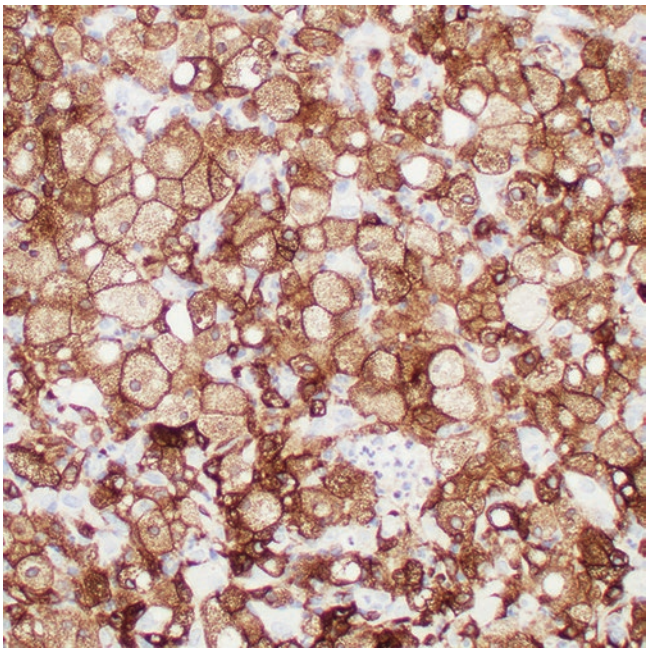

**Fig. 7.33** Expression of CD68 by immunohistochemical staining highlights the histiocytic nature of juvenile xanthogranuloma

## References

1. Favara BE, Feller AC, Pauli M, et al. Contemporary classification of histiocytic disorders. The WHO Committee on histiocytic/reticulum cell proliferations. Reclassification Working Group of the Histiocyte Society. Med Pediatr Oncol. 1997;29:157–66.
2. McClain KL, Natkunam Y, Swerdlow SH. Atypical cellular disorders. Hematology Am Soc Hematol Educ Program. 2004:283–96.
3. Wang CW, Colby TV. Histiocytic lesions and proliferations in the lung. Semin Diagn Pathol. 2007;24:162–82.
4. Katz SI, Tamaki K, Sachs DH. Epidermal Langerhans cells are derived from cells originating in bone marrow. Nature. 1979;282:324–6.
5. Howarth DM, Gilchrist GS, Mullan BP, et al. Langerhans cell histiocytosis: diagnosis, natural history, management, and outcome. Cancer. 1999;85:2278–90.
6. Basset F, Corrin B, Spencer H, et al. Pulmonary histiocytosis X. Am Rev Respir Dis. 1978;118:811–20.
7. Friedman PJ, Liebow AA, Sokoloff J. Eosinophilic granuloma of lung. Clinical aspects of primary histiocytosis in the adult. Medicine (Baltimore). 1981;60:385–96.
8. Aricò M, Egeler RM. Clinical aspects of Langerhans cell histiocytosis. Hematol Oncol Clin North Am. 1998;12:247–58.
9. Lieberman PH, Jones CR, Steinman RM, et al. Langerhans cell (eosinophilic) granulomatosis. A clinicopathologic study encompassing 50 years. Am J Surg Pathol. 1996;20:519–52.
10. Colby TV, Lombard C. Histiocytosis X in the lung. Hum Pathol. 1983;14:847–56.
11. Badalian-Very G, Vergilio JA, Degar BA, et al. Recurrent BRAF mutations in Langerhans cell histiocytosis. Blood. 2010;116:1919–23.
12. Yousem SA, Dacic S, Nikiforov YE, et al. Pulmonary Langerhans cell histiocytosis: profiling of multifocal tumors using next-generation sequencing identifies concordant occurrence of BRAF V600E mutations. Chest. 2013;143:1679–84.
13. Mason RH, Foley NM, Branley HM, et al. Pulmonary Langerhans cell histiocytosis (PLCH): a new UK register. Thorax. 2014;69:766–7.
14. Vassallo R, Limper AH. Pulmonary Langerhans' cell histiocytosis. Semin Respir Crit Care Med. 2002;23:93–101.
15. Travis WD, Borok Z, Roum JH, et al. Pulmonary Langerhans cell granulomatosis (histiocytosis X). A clinicopathologic study of 48 cases. Am J Surg Pathol. 1993;17:971–86.

16. Crausman RS, Jennings CA, Tuder RM, et al. Pulmonary histiocytosis X: pulmonary function and exercise pathophysiology. Am J Respir Crit Care Med. 1996;153:426–35.
17. Mendez JL, Nadrous HF, Vassallo R, et al. Pneumothorax in pulmonary Langerhans cell histiocytosis. Chest. 2004;125:1028–32.
18. Elia D, Torre O, Cassandro R, et al. Pulmonary Langerhans cell histiocytosis: a comprehensive analysis of 40 patients and literature review. Eur J Intern Med. 2015;26:351–6.
19. Brauner MW, Grenier P, Mouelhi MM, et al. Pulmonary histiocytosis X: evaluation with high-resolution CT. Radiology. 1989;172:255–8.
20. Brauner MW, Grenier P, Tijani K, et al. Pulmonary Langerhans cell histiocytosis: evolution of lesions on CT scans. Radiology. 1997;204:497–502.
21. Moore AD, Godwin JD, Müller NL, et al. Pulmonary histiocytosis X: comparison of radiographic and CT findings. Radiology. 1989;172:249–54.
22. Mogulkoc N, Veral A, Bishop PW, et al. Pulmonary Langerhans' cell histiocytosis: radiologic resolution following smoking cessation. Chest. 1999;115:1452–5.
23. Popper HH. Pulmonary Langerhans cell histiocytosis. Pathologe. 2015;36:451–7.
24. Schönfeld N, Frank W, Wenig S, et al. Clinical and radiologic features, lung function and therapeutic results in pulmonary histiocytosis X. Respiration. 1993;60:38–44.
25. Etienne B, Bertocchi M, Gamondes JP, et al. Relapsing pulmonary Langerhans cell histiocytosis after lung transplantation. Am J Respir Crit Care Med. 1998;157:288–91.
26. Dauriat G, Mal H, Thabut G, et al. Lung transplantation for pulmonary langerhans' cell histiocytosis: a multicenter analysis. Transplantation. 2006;81:746–50.
27. Le Pavec J, Lorillon G, Jaïs X, et al. Pulmonary Langerhans cell histiocytosis-associated pulmonary hypertension: clinical characteristics and impact of pulmonary arterial hypertension therapies. Chest. 2012;142:1150–7.
28. Delobbe A, Durieu J, Duhamel A, et al. Determinants of survival in pulmonary Langerhans' cell granulomatosis (histiocytosis X). Groupe d'Etude en Pathologie Interstitielle de la Société de Pathologie Thoracique du Nord. Eur Respir J. 1996;9:2002–6.
29. Naumann R, Beuthien-Baumann B, Fischer R, et al. Simultaneous occurrence of Hodgkin's lymphoma and eosinophilic granuloma: a potential pitfall in positron emission tomography imaging. Clin Lymphoma. 2002;3:121–4.
30. Burns BF. Molecular genetic markers in lymphoproliferative disorders. Clin Biochem. 1989;22:33–9.
31. Lombard CM, Medeiros LJ, Colby TV. Pulmonary histiocytosis X and carcinoma. Arch Pathol Lab Med. 1987;111:339–41.
32. Brody AR, Kanich RE, Graham WG, et al. Cyst wall formation in pulmonary eosinophilic granuloma. Chest. 1974;66:576–8.
33. Fartoukh M, Humbert M, Capron F, et al. Severe pulmonary hypertension in histiocytosis X. Am J Respir Crit Care Med. 2000;161:216–23.
34. Auerswald U, Barth J, Magnussen H. Value of CD-1-positive cells in bronchoalveolar lavage fluid for the diagnosis of pulmonary histiocytosis X. Lung. 1991;169:305–9.
35. Sholl LM, Hornick JL, Pinkus JL, et al. Immunohistochemical analysis of langerin in langerhans cell histiocytosis and pulmonary inflammatory and infectious diseases. Am J Surg Pathol. 2007;31:947–52.
36. Birbeck MS, Breathnach AS, Everall JD. An electron microscope study of basal melanocytes and high-level clear cells (Langerhans cells) in vitiligo. J Invest Dermatol. 1961;37:51–64.
37. Chester W. Über Lipoidgranulomatose. Virchows Arch Pathol Anat. 1930;279:561–602.
38. Veyssier-Belot C, Cacoub P, Caparros-Lefebvre D, et al. Erdheim-Chester disease. Clinical and radiologic characteristics of 59 cases. Medicine (Baltimore). 1996;75:157–69.
39. Shamburek RD, Brewer HB Jr, Gochuico BR. Erdheim-Chester disease: a rare multisystem histiocytic disorder associated with interstitial lung disease. Am J Med Sci. 2001;321:66–75.
40. Allen TC, Chevez-Barrios P, Shetlar DJ, et al. Pulmonary and ophthalmic involvement with Erdheim-Chester disease: a case report and review of the literature. Arch Pathol Lab Med. 2004;128:1428–31.
41. Haroche J, Charlotte F, Arnaud L, et al. High prevalence of BRAF V600E mutations in Erdheim-Chester disease but not in other non-Langerhans cell histiocytoses. Blood. 2012;120:2700–3.
42. Haroche J, Cohen-Aubart F, Emile JF, et al. Dramatic efficacy of vemurafenib in both multisystemic and refractory Erdheim-Chester disease and Langerhans cell histiocytosis harboring the BRAF V600E mutation. Blood. 2013;121:1495–500.
43. Ahuja J, Kanne JP, Meyer CA, et al. Histiocytic disorders of the chest: imaging findings. Radiographics. 2015;35:357–70.
44. Allen TC. Pulmonary Langerhans cell histiocytosis and other pulmonary histiocytic diseases: a review. Arch Pathol Lab Med. 2008;132:1171–81.
45. Mazor RD, Manevich-Mazor M, Shoenfeld Y. Erdheim-Chester disease: a comprehensive review of the literature. Orphanet J Rare Dis. 2013;8:137.
46. Arnaud L, Hervier B, Néel A, et al. CNS involvement and treatment with interferon-α are independent prognostic factors in Erdheim-Chester disease: a multicenter survival analysis of 53 patients. Blood. 2011;117:2778–82.
47. Hervier B, Arnaud L, Charlotte F, et al. Treatment of Erdheim-Chester disease with long-term high-dose interferon-α. Semin Arthritis Rheum. 2012;41:907–13.
48. Rush WL, Andriko JA, Galateau-Salle F, et al. Pulmonary pathology of Erdheim-Chester disease. Mod Pathol. 2000;13:747–54.
49. Egan AJ, Boardman LA, Tazelaar HD, et al. Erdheim-Chester disease: clinical, radiologic, and histopathologic findings in five patients with interstitial lung disease. Am J Surg Pathol. 1999;23:17–26.
50. Rosai J, Dorfman RF. Sinus histiocytosis with massive lymphadenopathy. A newly recognized benign clinicopathological entity. Arch Pathol. 1969;87:63–70.
51. Foucar E, Rosai J, Dorfman R. Sinus histiocytosis with massive lymphadenopathy (Rosai-Dorfman disease): review of the entity. Semin Diagn Pathol. 1990;7:19–73.
52. Cartin-Ceba R, Golbin JM, Yi ES, et al. Intrathoracic manifestations of Rosai-Dorfman disease. Respir Med. 2010;104:1344–9.
53. Ali A, Mackay D. Rosai-Dorfman disease of the lung. Thorax. 2009;64:908–9.
54. Roberts SS, Attanoos RL. IgG4+ Rosai-Dorfman disease of the lung. Histopathology. 2010;56:662–4.
55. Shi SS, Sun YT, Guo L. Rosai-Dorfman disease of lung: a case report and review of the literatures. Chin Med J. 2009; 122:873–4.
56. Ji H, Zhang B, Tian D, et al. Rosai-Dorfman disease of the lung. Respir Care. 2012;57:1679–81.
57. Noguchi S, Yatera K, Shimajiri S, et al. Intrathoracic Rosai-Dorfman disease with spontaneous remission: a clinical report and a review of the literature. Tohoku J Exp Med. 2012;227:231–325.
58. Imielski BR, Ramalingam VS, Rao RN, et al. Intrathoracic rosai-dorfman disease: hemorrhage with routine diagnostic procedure. Ann Thorac Surg. 2014;98:1459–61.
59. Hasegawa M, Sakai F, Okabayashi A, et al. Rosai-Dorfman disease of the lung overlapping with IgG4-related disease: the difficulty in its differential diagnosis. Intern Med. 2017;56:937–41.
60. El-Kersh K, Perez RL, Guardiola J. Pulmonary IgG4+ Rosai-Dorfman disease. BMJ Case Rep. 2013;2013.
61. Campana M, Goupil de Buille J, de Muret A, et al. Pulmonary manifestations revealing Rosai-Dorfman disease. Sarcoidosis Vasc Diffuse Lung Dis. 2015;32:275–7.

62. de Jong WK, Kluin PM, Groen HM. Overlapping immunoglobulin G4-related disease and Rosai-Dorfman disease mimicking lung cancer. Eur Respir Rev. 2012;21:365–7.
63. Zhang X, Hyjek E, Vardiman J. A subset of Rosai-Dorfman disease exhibits features of IgG4-related disease. Am J Clin Pathol. 2013;139:622–32.
64. Liu L, Perry AM, Cao W, et al. Relationship between Rosai-Dorfman disease and IgG4-related disease: study of 32 cases. Am J Clin Pathol. 2013;140:395–402.
65. Pulsoni A, Anghel G, Falcucci P, et al. Treatment of sinus histiocytosis with massive lymphadenopathy (Rosai-Dorfman disease): report of a case and literature review. Am J Hematol. 2002;69:67–71.
66. Syed A, Malhotra R, Shojaee S, et al. Exophytic tracheal mass. A rare presentation of Rosai-Dorfman disease. Ann Am Thorac Soc. 2013;10:518–20.
67. Prendes BL, Brinkman WT, Sengupta AL, et al. Atypical presentation of extranodal Rosai-Dorfman disease. Ann Thorac Surg. 2009;87:616–8.
68. Walters DM, Dunnington GH, Dustin SM, et al. Rosai-Dorfman disease presenting as a pulmonary artery mass. Ann Thorac Surg. 2010;89:300–2.
69. Scott JV, Henderson MH, Spradley CD. Extranodal Rosai-Dorfman disease presenting as hemoptysis: a case report. Chest. 2010;138:119A.
70. Apperley ST, Hyjek EM, Musani R, et al. Intrathoracic Rosai Dorfman disease with focal aggregates of IgG4-bearing plasma cells. Case report and literature review. Ann Am Thorac Soc. 2016;13:666–70.
71. Boissière L, Patey M, Toubas O, et al. Tracheobronchial involvement of Rosai-Dorfman disease: case report and review of the literature. Medicine (Baltimore). 2016;95:e2821.
72. Köksal D, Ozcan A, Demirağ F, et al. Pulmonary malakoplakia: a case report and review of the literature. Tuberk Toraks. 2014;62:248–52.
73. Michaelis L. Über Einschlüsse in Blasentumoren. Z Kiln Med. 1902;47:208–15.
74. Von Hansemann D. Über Malakoplakie der Harnblase. Virchows Arch. 1903;173:302–8.
75. Stanton MJ, Maxted W. Malacoplakia: a study of the literature and current concepts of pathogenesis, diagnosis and treatment. J Urol. 1981;125:139–46.
76. Colby TV, Hunt S, Pelzmann K, et al. Malakoplakia of the lung: a report of two cases. Respiration. 1980;39:295–9.
77. Mandal P, Wallace WA, Skwarski KM. Pulmonary malakoplakia: a rare presentation mimicking extensive stage IV lung cancer. Eur Respir J. 2011;38:983–5.
78. Mulè A, Petrone G, Santoro A, et al. Pulmonary malacoplakia at early stage: use of polymerase chain reaction for detection of Rhodococcus equi. Int J Immunopathol Pharmacol. 2012;25:703–12.
79. Kwon KY, Colby TV. Rhodococcus equi pneumonia and pulmonary malakoplakia in acquired immunodeficiency syndrome. Pathologic features. Arch Pathol Lab Med. 1994;118:744–8.
80. Scott MA, Graham BS, Verrall R, et al. Rhodococcus equi--an increasingly recognized opportunistic pathogen. Report of 12 cases and review of 65 cases in the literature. Am J Clin Pathol. 1995;103:649–55.
81. Whipple GH. A hitherto undescribed disease characterized anatomically by deposits of fat and fatty acids in the intestinal and mesenteric lymphatic tissues. Bull Johns Hopkins Hosp. 1907;18:382–91.
82. Relman DA, Schmidt TM, MacDermott RP, et al. Identification of the uncultured bacillus of Whipple's disease. N Engl J Med. 1992;327:293–301.
83. Fenollar F, Trani M, Davoust B, et al. Prevalence of asymptomatic Tropheryma whipplei carriage among humans and nonhuman primates. J Infect Dis. 2008;197:880–7.
84. Lagier JC, Fenollar F, Lepidi H, et al. Evidence of lifetime susceptibility to Tropheryma whipplei in patients with Whipple's disease. J Antimicrob Chemother. 2011;66:1188–9.
85. Fenollar F, Puéchal X, Raoult D. Whipple's disease. N Engl J Med. 2007;356:55–66.
86. Urbanski G, Rivereau P, Artru L, et al. Whipple disease revealed by lung involvement: a case report and literature review. Chest. 2012;141:1595–8.
87. Kelly CA, Egan M, Rawlinson J. Whipple's disease presenting with lung involvement. Thorax. 1996;51:343–4.
88. Cho C, Linscheer WG, Hirschkorn MA, et al. Sarcoidlike granulomas as an early manifestation of Whipple's disease. Gastroenterology. 1984;87:941–7.
89. Symmons DP, Shepherd AN, Boardman PL, et al. Pulmonary manifestations of Whipple's disease. Q J Med. 1985;56:497–504.
90. Dzirlo L, Hubner M, Müller C, et al. A mimic of sarcoidosis. Lancet. 2007;369:1832.
91. Puéchal X. Whipple's disease. Ann Rheum Dis. 2013;72:797–803.
92. Canessa PA, Pratticò L, Sivori M, et al. Acute fibrinous and organising pneumonia in Whipple's disease. Monaldi Arch Chest Dis. 2008;69:186–8.
93. Arnold CA, Moreira RK, Lam-Himlin D, et al. Whipple disease a century after the initial description: increased recognition of unusual presentations, autoimmune comorbidities, and therapy effects. Am J Surg Pathol. 2012;36:1066–73.
94. Yamamoto T, Hishida A, Honda N, et al. Crystal-storing histiocytosis and crystalline tissue deposition in multiple myeloma. Arch Pathol Lab Med. 1991;115:351–4.
95. Kapadia SB, Enzinger FM, Heffner DK, et al. Crystal-storing histiocytosis associated with lymphoplasmacytic neoplasms. Report of three cases mimicking adult rhabdomyoma. Am J Surg Pathol. 1993;17:461–7.
96. Dogan S, Barnes L, Cruz-Vetrano WP. Crystal-storing histiocytosis: report of a case, review of the literature (80 cases) and a proposed classification. Head Neck Pathol. 2012;6:111–20.
97. Papla B, Spólnik P, Rzenno E, et al. Generalized crystal-storing histiocytosis as a presentation of multiple myeloma: a case with a possible pro-aggregation defect in the immunoglobulin heavy chain. Virchows Arch. 2004;445:83–9.
98. Pitman SD, Wang J, Serros ER, et al. A 70-year-old woman with acute renal failure. Crystal-storing histiocytosis. Arch Pathol Lab Med. 2006;130:1077–8.
99. Rossi G, De Rosa N, Cavazza A, et al. Localized pleuropulmonary crystal-storing histiocytosis: 5 cases of a rare histiocytic disorder with variable clinicoradiologic features. Am J Surg Pathol. 2013;37:906–12.
100. Lebeau A, Zeindl-Eberhart E, Müller EC, et al. Generalized crystal-storing histiocytosis associated with monoclonal gammopathy: molecular analysis of a disorder with rapid clinical course and review of the literature. Blood. 2002;100:1817–27.
101. Fairweather PM, Williamson R, Tsikleas G. Pulmonary extranodal marginal zone lymphoma with massive crystal storing histiocytosis. Am J Surg Pathol. 2006;30:262–7.
102. Zhang C, Myers JL. Crystal-storing histiocytosis complicating primary pulmonary marginal zone lymphoma of mucosa-associated lymphoid tissue. Arch Pathol Lab Med. 2013;137:1199–204.
103. Prasad ML, Charney DA, Sarlin J, et al. Pulmonary immunocytoma with massive crystal storing histiocytosis: a case report with review of literature. Am J Surg Pathol. 1998;22:1148–53.
104. Jones D, Renshaw AA. Recurrent crystal-storing histiocytosis of the lung in a patient without a clonal lymphoproliferative disorder. Arch Pathol Lab Med. 1996;120:978–80.

105. Ionescu DN, Pierson DM, Qing G, et al. Pulmonary crystal-storing histiocytoma. Arch Pathol Lab Med. 2005;129:1159–63.
106. Amir G, Ron N. Pulmonary pathology in Gaucher's disease. Hum Pathol. 1999;30:666–70.
107. Nicholson AG, Florio R, Hansell DM, et al. Pulmonary involvement by Niemann-Pick disease. A report of six cases. Histopathology. 2006;48:596–603.
108. Brown LK, Miller A, Bhuptani A, et al. Pulmonary involvement in Fabry disease. Am J Respir Crit Care Med. 1997;155:1004–10.
109. Schneider EL, Epstein CJ, Kaback MJ, et al. Severe pulmonary involvement in adult Gaucher's disease. Report of three cases and review of the literature. Am J Med. 1977;63:475–80.
110. Eng CM, Germain DP, Banikazemi M, et al. Fabry disease: guidelines for the evaluation and management of multi-organ system involvement. Genet Med. 2006;8:539–48.
111. Minai OA, Sullivan EJ, Stoller JK. Pulmonary involvement in Niemann-Pick disease: case report and literature review. Respir Med. 2000;94:1241–51.
112. Vellodi A, Hobbs JR, O'Donnell NM, et al. Treatment of Niemann-Pick disease type B by allogeneic bone marrow transplantation. Br Med J (Clin Res Ed). 1987;295:1375–6.
113. Kim W, Pyeritz RE, Bernhardt BA, et al. Pulmonary manifestations of Fabry disease and positive response to enzyme replacement therapy. Am J Med Genet A. 2007;143:377–81.
114. Renapurkar RD, Kanne JP. Metabolic and storage lung diseases: spectrum of imaging appearances. Insights Imaging. 2013;4:773. [Epub ahead of print].
115. Skikne MI, Prinsloo I, Webster I. Electron microscopy of lung in Niemann-Pick disease. J Pathol. 1972;106:119–22.
116. Andrianopoulos E, Lautides G, Kormas P, et al. Pulmonary xanthoma. A case report with immunohistologic study and DNA-image analysis. Eur J Cardiothorac Surg. 1995;9:534–6.
117. Murphy JT, Soeken T, Megison S, et al. Juvenile xanthogranuloma: diverse presentations of noncutaneous disease. J Pediatr Hematol Oncol. 2014;36:641–5.
118. Bakir B, Unuvar E, Terzibasioglu E, et al. Atypical lung involvement in a patient with systemic juvenile xanthogranuloma. Pediatr Radiol. 2007;37:325–7.
119. Lin L, Salisbury EL, Gardiner I, et al. Solitary juvenile xanthogranuloma in the lung of a young adult. Pathology. 2011;43:503–7.
120. Fisher ER, Beyer FD. Postinflammatory tumor (xanthoma) of lung. Dis Chest. 1959;36:43–8.
121. Schwartz EE, Katz SM, Mandell GA. Postinflammatory pseudotumors of the lung: fibrous histiocytoma and related lesions. Radiology. 1980;136:609–13.
122. Pearl M, Woolley MM. Pulmonary xanthomatous postinflammatory pseudotumors in children. J Pediatr Surg. 1973;8:255–61.
123. Greenberg SD, Jenkins DE. Xanthomatous inflammatory pseudotumor of the lung. South Med J. 1975;68:754–6.
124. Carter R, Wareham EE, Bullock WK, et al. Intrathoracic fibroxanthomatous pseudotumors: report of 10 cases and review of the literature. Ann Thorac Surg. 1968;5:97–111.
125. Kraus MD, Haley JC, Ruiz R, et al. "Juvenile" xanthogranuloma: an immunophenotypic study with a reappraisal of histogenesis. Am J Dermatopathol. 2001;23:104–11.
126. Freyer DR, Kennedy R, Bostrom BC, et al. Juvenile xanthogranuloma: forms of systemic disease and their clinical implications. J Pediatr. 1996;129:227–37.
127. Dehner LP. Juvenile xanthogranulomas in the first two decades of life: a clinicopathologic study of 174 cases with cutaneous and extracutaneous manifestations. Am J Surg Pathol. 2003;27:579–93.